# Coordinative Unsaturation in Chiral Organolanthanides. Synthetic and Asymmetric Catalytic Mechanistic Study of Organoyttrium and -lutetium Complexes Having Pseudo-*meso* $Me_2Si(\eta^5\text{-}RC_5H_3)(\eta^5\text{-}R^*C_5H_3)$ Ancillary Ligation[1]

Christopher M. Haar, Charlotte L. Stern, and Tobin J. Marks*

*Department of Chemistry, Northwestern University, Evanston, Illinois 60208-3113*

*Received November 7, 1995*[⊗]

As established by NMR, circular dichroism, and X-ray diffraction, organolanthanide complexes of the new chelating ligand $Me_2Si(3\text{-}Me_3SiCp)[3\text{-}(-)\text{-menthylCp}]^{2-}$ ($Cp = \eta^5\text{-}C_5H_3$) preferentially adopt a single planar chiral configuration of the asymmetric metal−ligand template. Chloro complexes $(S,R)\text{-}Me_2Si(Me_3SiCp)[(-)\text{-menthylCp}]Ln(\mu\text{-}Cl)_2Li(OEt_2)_2$ (Ln = Y, Lu) were isolated diastereomerically pure by crystallization from diethyl ether. The unusual pseudo-*meso* configuration leads to a gross distortion from ideal $C_{2v}$ symmetry, evidenced by a significant deviation of $\angle Si_{bridge}-Lu-Li$ from linearity (158°). At least two additional epimers are detected in THF solution. Alkylation of the (*S*,*R*) epimers with $LiCH(SiMe_3)_2$ proceeds with retention of configuration, affording chiral hydrocarbyl complexes in quantitative yield. In solution, the hydrocarbyls exhibit temperature-dependent conformational exchange processes in the NMR ascribable to restricted rotation about the $Ln-CH(SiMe_3)_2$ bond. These complexes are effective precatalysts for asymmetric hydrogenation of unfunctionalized olefins and for the reductive cyclization of 1,5-dienes. The highest enantioselectivities are obtained when the Lu complex is used for hydrogenation of 2-phenyl-1-butene (45% ee) and deuteration of styrene (10% ee) and 1-pentene (30% ee). The hydrogenation of 2-phenyl-1-butene with the Y catalyst (yielding exclusively 2-phenylbutane-1,2-$d_2$ under $D_2$) obeys a rate law of the approximate form $v = (k[\text{olefin}]^1[\text{lanthanide}]^{1/2}[H_2]^1)/(K + [\text{olefin}])$, suggesting rapid, operationally irreversible olefin insertion at a putative hydride, a rapid preequilibrium involving an alkyl or alkyl/hydride dimer, and turnover-limiting hydrogenolysis of an intermediate yttrium alkyl with $v_{H_2}/v_{D_2} = 2.2 \pm 0.1$. The apparent rate constant for 2-phenyl-1-butene hydrogenation ($12(1) \times 10^{-3}$ $M^{1/2}$ $atm^{-1}$ $s^{-1}$) is ca. 1 order of magnitude lower than for chiral $Me_2Si(Me_4C_5)(3\text{-}R^*Cp)Ln$-based systems (R* = (−)-menthyl, (+)-neomenthyl; Ln = Y, La, Nd, Sm, Lu), principally reflecting diminished Ln−C bond hydrogenolytic reactivity.

Downloaded by CARLI CONSORTIUM on June 30, 2009
Published on April 2, 1996 on http://pubs.acs.org | doi: 10.1021/om950871v

The successful development of organometallic catalysts for asymmetric organic transformations relies to a great extent on the evolution of ancillary ligation which preserves or beneficially alters the activity of an established catalytic system while enforcing the desired chiral outcome of a particular reaction. Over the past 30 years, chiral metal complexes—predominantly of the late transition series—have increasingly displayed a remarkable utility as selective catalysts for a variety of asymmetric transformations.[2]

More recently, this same strategy has been shrewdly applied to the development of chiral early transition metallocene catalyst systems $(CpR^*)_2MCl_2$ (M = Ti, Zr; Cp = cyclopentadienyl-type ligand; R* = chiral auxiliary)[3] and $X(CpR)_2MCl_2$ (M = Ti, Zr, Hf; X = $Me_2Si$, $(CH_2)_2$, $(CH_2)_3$, etc.).[4] Although such catalyst systems have been applied to asymmetric olefin,[3,5] imine,[6] and ketone[7] hydrogenation, they are known primarily for the stereoregular polymerization of α-olefins[8] and, more recently, the cyclopolymerization of α,ω-diolefins.[9] With few exceptions,[3a] these catalyst systems rely on the presence of a $C_2$-symmetric ligand or metal−ligand array, the stereoselective synthesis of which typically

⊗ Abstract published in *Advance ACS Abstracts,* March 1, 1996.

(1) Communicated in part: Haar, C. M.; Stern, C. L.; Marks, T. J. *Abstracts of Papers,* 207th National Meeting of the American Chemical Society, San Diego, CA, 1994, INOR 42.

(2) For leading references in asymmetric homogeneous catalysis, see: (a) Noyori, R. *Asymmetric Catalysis in Organic Synthesis*; Wiley: New York, 1994. (b) Pfaltz, A. *Acc. Chem. Res.* **1993**, *26*, 339−345. (c) *Chem. Rev.* **1992**, 92, 739−1140. This entire issue is dedicated to enantioselective synthesis. (d) Parshall, G. W.; Ittel, S. D. *Homogeneous Catalysis,* 2nd ed.; Wiley: New York, 1992; Chapters 2, 3, and 6. (e) Noyori, R. *Chem. Soc. Rev.* **1989**, *18*, 187−208. (f) Scott, J. W. *Top. Stereochem.* **1989**, *19*, 209−225. (g) Brunner, H. *Synthesis* **1988**, 645−654. (h) Bosnich, B. *Asymmetric Catalysis*; NATO ASI Series E 103; Martinus Nijhoff Publishers: Dordrecht, The Netherlands, 1986. (i) *Asymmetric Synthesis*; Morrison, J. D., Ed.; Academic Press: New York, 1985; Vol. 5.

(3) (a) Erker, G.; Aulbach, M.; Krueger, C.; Werner, S. *J. Organomet. Chem.* **1993**, *450*, 1−7. (b) Halterman, R. L. *Chem. Rev.* **1992**, *92*, 965−994. (c) Moriarty, K. J.; Rogers, R. D.; Paquette, L. A. *Organometallics* **1989**, *8*, 1512−1517. (d) Paquette, L. A.; Moriarty, K. J.; Rogers, R. D. *Organometallics* **1989**, *8*, 1506−1511. (e) Paquette, L. A.; Moriarty, K. J.; McKinney, J. A.; Rogers, R. D. *Organometallics* **1989**, *8*, 1707−1713. (f) Halterman, R. L.; Vollhardt, K. P. C. *Organometallics* **1988**, *7*, 883−892. (g) Halterman, R. L.; Vollhardt, K. P. C.; Welker, M. E.; Bläser, D.; Boese, R. *J. Am. Chem. Soc.* **1987**, *109*, 8105−8107. (h) Paquette, L. A.; McKinney, J. A.; McLaughlin, M. L.; Rheingold, A. L. *Tetrahedron Lett.* **1986**, *27*, 5599−5602. (i) Halterman, R. L.; Vollhardt, K. P. C. *Tetrahedron Lett.* **1986**, *27*, 1461−1464. (j) Dormond, A.; El Bouadili, A.; Moise, C. *Tetrahedron. Lett.* **1983**, *24*, 3087−3089. (k) Couturier, S.; Tainturier, G.; Gautheron, B. *J. Organomet. Chem.* **1980**, *195*, 291−306. (l) Le Blanc, J. C.; Moise, C.; Tirouflet, J. *J. Organomet. Chem.* **1978**, *148*, 171−178. (m) Cesarotti, E.; Kagan, H. B.; Goddard, R.; Kruger, C. *J. Organomet. Chem.* **1978**, *162*, 297−309. (n) Le Blanc, J. C.; Moise, C. *J. Organomet. Chem.* **1976**, *120*, 65−71.

0276-7333/96/2315-1765$12.00/0 © 1996 American Chemical Society

involves one or more discrete resolution steps, either during the synthesis of the ligand or, in the case of the *ansa* metallocenes $X(CpR)_2MCl_2$, after complexation to the metal. In the latter case, not only must undesired *meso* isomers[10] (**5**) be removed from the reaction mixture but the enantiomers (**6**) must also be resolved to obtain homochiral catalysts.[11]

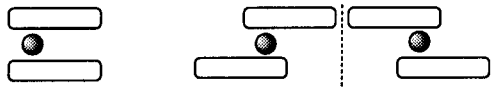

*meso* **5** *rac* **6**

The organolanthanide hydrides[12] $(Cp'_2LnH)_2$[13,14] and $(Me_2SiCp''_2LnH)_2$[15] ($Cp' = \eta^5$-$Me_5C_5$, $Cp'' = \eta^5$-$Me_4C_5$) have proven to be highly efficient catalysts for a variety of olefin transformations including hydrogenation,[16] oligomerization/polymerization,[13a,b,14,15,17,18] isomerization,[19] hydroamination,[20] hydrosilylation,[21] hydrophosphination,[22] hydroboration,[23] and reductive or silylative cyclization of $\alpha,\omega$-dienes.[24] Only recently, however, have investigators begun to explore asymmetric ancillary ligation designed to exploit the intrinsic high reactivity of the lanthanide metallocenes in enantioselective catalysis.[25,26]

Reports from this laboratory have detailed the characteristics of $Me_2SiCp''(CpR^*)$ ($Cp'' = \eta^5$-$Me_4C_5$; R* = (+)-neomenthyl, (−)-menthyl, (+)-phenylmenthyl) supporting ligation in the diastereoselective synthesis of $C_1$-symmetric organolanthanide catalysts capable of effecting moderate to high (up to 96% ee) enantioselectivities in the catalytic hydrogenation of styrenic olefins as well as in the hydroamination/cyclization of a variety of amino−olefins.[26] The design strategy (**7**, **8**) is a modification of existing ring-linked cyclopentadienyl f-element systems[13b,27] into which a chirally-substituted

Downloaded by CARLI CONSORTIUM on June 30, 2009
Published on April 2, 1996 on http://pubs.acs.org | doi: 10.1021/om950871v

(4) (a) Grossman, R. B.; Tsai, J.-C.; Davis, W. M.; Gutierrez, A.; Buchwald, S. L. *Organometallics* **1994**, *13*, 3892−3896. (b) Röll, W.; Brintzinger, H.-H.; Rieger, B.; Zolk, R. *Angew. Chem., Int. Ed. Engl.* **1990**, *29*, 279−280. (c) Burger, P.; Hund, H.-U.; Evertz, K.; Brintzinger, H. H. *J. Organomet. Chem.* **1989**, *370*, 153−161. (d) Wiesenfeldt, H.; Reinmuth, A.; Barsties, E.; Evertz, K.; Brintzinger, H. H. *J. Organomet. Chem.* **1989**, *369*, 359−370. (e) Gutmann, S.; Burger, P.; Hund, H. U.; Hofmann, J.; Brintzinger, H. H. *J. Organomet. Chem.* **1989**, *369*, 343−357. (f) Ewen, J. A.; Haspeslagh, L.; Atwood, J. L.; Zhang, H. *J. Am. Chem. Soc.* **1987**, *109*, 6544−6545. (g) Röll, W.; Zsolnai, L.; Hüttner, G.; Brintzinger, H.-H. *J. Organomet. Chem.* **1987**, *322*, 65−70. (h) Wild, F. R. W. P.; Wasiucionek, M.; Hüttner, G.; Brintzinger, H.-H. *J. Organomet. Chem.* **1985**, *288*, 63−67. (i) Schwemlein, H.; Brintzinger, H. H. *J. Organomet. Chem.* **1983**, *254*, 69−73.

(5) (a) Broene, Richard D.; Buchwald, Stephen L. *J. Am. Chem. Soc.* **1993**, *115*, 12569−12570. (b) Grossman, R. B.; Doyle, R. A.; Buchwald, S. L. *Organometallics* **1991**, *10*, 1501−1505. (c) Waymouth, Robert; Pino, P. *J. Am. Chem. Soc.* **1990**, *112*, 4911−4914.

(6) (a) Willoughby, C. A.; Buchwald, S. L. *J. Am. Chem. Soc.* **1994**, *116*, 11703−11714. (b) Lee, N. E.; Buchwald, S. L. *J. Am. Chem. Soc.* **1994**, *116*, 5985−6. (c) Willoughby, C. A.; Buchwald, S. L. *J. Org. Chem.* **1993**, *58* (27), 7627−9. (d) Willoughby, C. A.; Buchwald, S. L. *J. Am. Chem. Soc.* **1992**, *114*, 7562−4.

(7) Carter, M. B.; Schiøtt, B.; Gutiérrez, A.; Buchwald, S. L. *J. Am. Chem. Soc.* **1994**, *116*, 11667−11670.

(8) (a) Spaleck, W.; Küber, F.; Winter, A.; Rohrmann, J.; Bachmann, B.; Antberg, M.; Dolle, V.; Paulus, E. F. *Organometallics* **1994**, *13*, 954. (b) Spaleck, W.; Antberg, M.; Rohrmann, J.; Winter, A.; Bachmann, B.; Kiprof, P.; Behm, J.; Herrmann, W. A. *Angew. Chem., Int. Ed. Engl.* **1992**, *31*, 1347. (c) Rieger, B. *J. Organomet. Chem.* **1992**, *428*, C33−C36. (d) Chien, J. C. W.; Tsai, W. M.; Rausch, M. D. *J. Am. Chem. Soc.* **1991**, *113*, 8570. (e) Erker, G.; Nolte, R.; Aul, R.; Wilker, S.; Kruger, C.; Noe, R. *J. Am. Chem. Soc.* **1991**, *113*, 7594−7602. (f) Röll, W.; Brintzinger, H. H.; Rieger, B.; Zolk, R. *Angew. Chem., Int. Ed. Engl.* **1990**, *29*, 279−280. (g) Rieger, B.; Mu, X.; Mallin, D. T.; Rausch, M. D.; Chien, J. C. W. *Macrmolecules* **1990**, *23*, 3559−3568. (h) Erker, G.; Nolte, R.; Tsay, Y.; Kruger, C. *Angew. Chem., Int. Ed. Engl.* **1989**, *28*, 628−629. (i) Ewen, J. A.; Haspeslagh, L.; Atwood, J. L.; Zhang, H. *J. Am. Chem. Soc.* **1987**, *109*, 6544−6545. (j) Kaminsky, W.; Kulper, K.; Niedoba, S. *Makrolmol. Chem., Macromol. Symp.* **1986**, *3*, 377−387. (k) Kaminsky, W.; Kulper, K.; Brintzinger, H. H.; Wild, F. R. W. P. *Angew. Chem., Int. Ed. Engl.* **1985**, *24*, 507−508. (l) Ewen, J. A. *J. Am. Chem. Soc.* **1984,** *106*, 6355−6364.

(9) Coates, G. W.; Waymouth, R. M. *J. Am. Chem. Soc.* **1993**, *115*, 91−98.

(10) (a) Rheingold, A. L.; Robinson, N. P.; Whelan, J.; Bosnich, B. *Organometallics* **1992**, *11*, 1869−1876. (b) Collins, S.; Hong, Y.; Ramachandran, R.; Taylor, N. J. *Organometallics* **1991**, *10*, 2349−2356. (c) Collins, S.; Gauthier, W. J.; Holden, D. A.; Kuntz, B. A.; Taylor, N. J.; Ward, D. G. *Organometallics* **1991**, *10*, 2061−2068. (d) Collins, S.; Hong, Y.; Taylor, N. J. *Organometallics* **1990**, *9*, 2695−2703. (e) Gutmann, S.; Burger, P.; Hund, H. U.; Hofmann, J.; Brintzinger, H. H. *J. Organomet. Chem.* **1989**, *369*, 343−357. (f) Wiesenfeldt, H.; Reinmuth, A.; Barsties, E.; Evertz, K.; Brintzinger, H. H. *J. Organomet. Chem.* **1989**, *369*, 359−370. (g) Wild, F. R. W. P.; Wasiucionek, M.; Hüttner, G.; Brintzinger, H. H. *J. Organomet. Chem.* **1985**, *228*, 63−67.

(11) (a) Schäfer, A.; Karl, E.; Zsolnai, L.; Hüttner, G.; Brintzinger, H. H. *J. Organomet. Chem.* **1987**, *328*, 87−99. (b) Wild, F. R. W. P.; Zsolnai, L.; Hüttner, G.; Brintzinger, H. H. *J. Organomet. Chem.* **1982**, *232*, 233−247.

(12) For comprehensive reviews of organolanthanide chemistry, see: (a) Schumann, H.; Messe-Marktscheffel, J.; Esser, L. *Chem. Rev.* **1995**, *95*, 865−869 and references therein. (b) Schaverien, C. J. *Adv. Organomet. Chem.* **1994**, *36*, 283−362 and references therein.

(13) (a) Heeres, H. J.; Renkema, J.; Booij, M.; Meetsma, A.; Teuben, J. H. *Organometallics* **1988**, *7*, 2495−2502. (b) den Haan, K. H.; de Boer, J. L.; Teuben, J. H.; Spek, A. L.; Kajic-Prodic, B.; Hays, G. R.; Huis, R. *Organometallics* **1986**, *5*, 1726−1733. (c) Jeske, G.; Lauke, H.; Mauermann, H.; Swepston, P. N.; Schumann, H.; Marks, T. J. *J. Am. Chem. Soc.* **1985**, *107*, 8091−8103. (d) Mauermann, H.; Swepston, P. N.; Marks, T. J. *Organometallics* **1985**, *4*, 200−202. (e) Watson, P. L.; Parshall, G. W. *Acc. Chem. Res.* **1985**, *18*, 51−55.

(14) For related $Cp'_2ScR$ complexes, see: (a) Burger, B. J.; Thompson, M. E.; Cotter, D. W.; Bercaw, J. E. *J. Am. Chem. Soc.* **1990**, *112*, 1566−1577. (b) Thompson, M. E.; Bercaw, J. E. *Pure Appl. Chem.* **1984**, *56*, 1−11.

(15) (a) Heeres, H. Ph.D. Thesis, University of Groningen, 1990. (b) Jeske, G.; Schock, L. E.; Swepston, P. N.; Schumann, H.; Marks, T. J. *J. Am. Chem. Soc.* **1985**, *107*, 8103−8110.

(16) (a) Molander, G. A.; Hoberg, J. O. *J. Org. Chem.* **1992**, *57*, 3266−3268. (b) Jeske, G.; Lauke, H.; Mauermann, H.; Schumann, H.; Marks, T. J. *J. Am. Chem. Soc.* **1985**, *107*, 8111−8118. (c) Evans, W. J.; Bloom, I.; Hunter, W. E.; Atwood, J. L. *J. Am. Chem. Soc.* **1983**, *105*, 1401−1403.

(17) (a) Watson, P. L.; Herskovitz, T. *ACS Symp. Ser.* **1983**, *No. 212*, 459−479. (b) Watson, P. L. *J. Am. Chem. Soc.* **1982**, *104*, 337−339. (c) Watson, P. L.; Roe, D. C. *J. Am. Chem. Soc.* **1982**, *104*, 6471−6473.

(18) Yang, X.; Seyam, A. M.; Fu, P.; Marks, T. J. *Macromolecules* **1994**, *27*, 4625−4626.

(19) $(Cp'_2LnH)_2$ and $(Me_2SiCp''_2NdH)_2$ also catalyze the isomerization of (*E*)-*N*,*N*-dimethyl-3-phenyl-2-butenylamine to (*E*)-*N*,*N*-dimethyl-3-phenyl-2-butenylamine at 80 °C in $C_6D_6$ (Conticello, V. P.; Giardello, M. A.; Eisen, M.; Marks, T. J., Unpublished results). For related Rh-catalyzed isomerizations of allylamines to enamines see: (a) Tani, K.; Yamagata, T.; Akutagawa, S.; Kumobayash; H.; Taketomi, T.; Takaya, H.; Miyashita, H.; Noyori, R.; Otsuka, S. *J. Am. Chem. Soc.* **1984**, *106*, 5208−5217. (b) Tani, K.; Yamagata, T.; Otsuka, S.; Akutagawa, S.; Kumobayashi, H.; Taketomi, T.; Takaya, H., Miyashita, A.; Noyori, R. *J. Chem. Soc., Chem. Commun.* **1982**, 600−601.

(20) (a) Gagné, M. R.; Stern, C.; Marks, T. J. *J. Am. Chem. Soc.* **1992**, *114*, 275−294. (b) Gagné, M. R.; Nolan, S. P.; Marks, T. J. *Organometallics* **1990**, *9*, 1716−1718. (c) Gagné, M. R.; Marks, T. J. *J. Am. Chem. Soc.* **1989**, *111*, 4108−4109. (d)

(21) (a) Fu, P.-F.; Marks, T. J. *J. Am. Chem. Soc.* **1995**, *117*, 10747−10748. (b) Fu, P.-F.; Brard, L.; Li, Y.; Marks, T. J. *J. Am. Chem. Soc.* **1995**, *117*, 7157−7168. (c) Molander, G. A.; Nichols, P. J. *J. Am. Chem. Soc.* **1995**, *117*, 4415−4416. (d) Molander, G. A.; Julius, M. *J. Org. Chem.* **1992**, *57*, 6347−6351. (e) Takahashi, T.; Hasegawa, M.; Suzuki, N.; Saburi, M.; Rousset, C. J.; Fanwick, P. E.; Negishi, E. *J. Am. Chem. Soc.* **1991**, *113*, 8564−8566. (f) Sakakura, T.; Lautenschlager, H.; Tanaka, M. *J. Chem. Soc., Chem. Commun.* **1991**, 40−41.

(22) Giardello, M. A.; King, W., A.; Nolan, S. P.; Porchia, M.; Sishta, C.; Marks, T. J. In *Energetics of Organometallic Species*; Martinho Simoes, J. A., Ed.; Kluwer: Dordrecht, The Netherlands, 1992; pp 35−51.

(23) (a) Harrison, K. N.; Marks, T. J. *J. Am. Chem. Soc.* **1992**, *114*, 9220−9221. (b) Bijpost, E. A.; Duchateau, R.; Teuben, J. H. *J. Mol. Catal.* **1995**, *95*, 121−128.

(24) (a) Molander, G. A.; Nichols, P. J. *J. Am. Chem. Soc.* **1995**, *117*, 4415−4416. (b) Molander, G. A.; Hoberg, J. O. *J. Am. Chem. Soc.* **1992**, *114*, 3123−3125.

(25) Coughlin, E. B.; Bercaw, J. E. *J. Am. Chem. Soc.* **1992**, *114*, 7606−7607.

(26) (a) Giardello, M. A. Sabat, M.; Rheingold, A. L.; Stern, C. L. *J. Am. Chem. Soc.* **1994**, *116*, 10212−10240. (b) Giardello, M. A.; Conticello, V. P.; Brard, L.; Gagné, M. R.; Marks, T. J. *J. Am. Chem. Soc.* **1994**, *116*, 10241−10254.

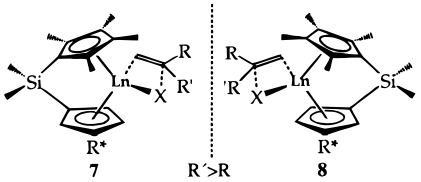


7 8

cyclopentadienyl group is incorporated. The attractions of such an approach are accessibility of resolvable, enantiomerically-related, chiral organolanthanide centers with cyclopentadienyl ligation capable, *via* lateral and vertical shape discrimination, of selectively differentiating between opposite enantiofaces of a prochiral substrate.

The results described here build upon this strategy and the resulting structure/reactivity data base[26] while taking advantage of the flexibility offered by cyclopentadienyl ligation in tuning metallocene selectivity and reactivity patterns through modifications in metal ionic radius and ring substitution.[13c,d,15b,20,26,27] The approach delineated in Scheme 1 offers an intermediate level of ring substitution/lanthanide coordinative unsaturation between the known $Me_2SiCp''(R^*Cp)LnR$ and $R_2SiCp''$-CpLnR complexes. The substitution motif mimics that of $X(CpR)_2MCl_2$-type complexes; however, inclusion of a chiral (−)-menthyl auxiliary (R*) allows for the possibility of four diastereomerically related, and therefore potentially separable, isomers. Steric considerations would *a priori* appear to favor pseudo-$C_2$-symmetric, diastereomeric configurations **11** and **12**. Note, however, that unlike analogous achiral $X(CpR)_2$ ligation, for which *meso* configurations (**5**) are achiral, diastereomers **9** and **10** are also chiral. Indeed, the disparate steric requirements of $Me_3Si$ and (−)-menthyl in the transverse plane, coupled with the lateral dissymmetry of the molecule, also provide a plausible and potentially instructive basis for enantioselection (**13**, **14**). Thus, isolation of any one of the four possible diastereomers provides a diastereomerically pure chiral catalyst requiring no further purification.[28]

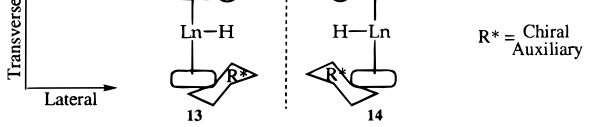


13 14

We present here a detailed synthetic, structural, and catalytic/mechanistic study of the **9**−**12** system where Ln = Y and Lu and R* = (−)-menthyl. We compare reactivity and catalytic behavior with that of the

**Scheme 1**

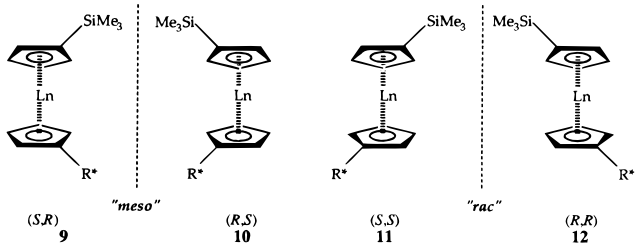


mechanistically well-characterized congeners $Cp'_2LnR$,[13,14,16] $Me_2SiCp''_2LnR$,[15] $R_2SiCp''CpLnR$,[27] $Me_2SiCp''(R^*Cp)LnR$,[26b] and $Cp'Y(OAr)R$[29] (OAr = $OC_6H_3$-$^tBu_2$-2,6; R = $CH(SiMe_3)_2$ or H). It will be seen that metal−ligand stereochemical and structural preferences in this series (**9**, **10** *vs.* **11**, **12**) are somewhat different from what might be expected on the basis of analogous $Sc^{3+}$ [14] and group 4 chemistry.[3,4,10,11] There are also substantial and informative differences in catalytic behavior *vis-à-vis* the other organolanthanide catalysts which reflect subtle changes in ancillary ligand structural and electronic characteristics.

## Experimental Section

**Materials and Methods.** All manipulations of air-sensitive materials were performed with the rigorous exclusion of oxygen and moisture in flamed Schlenk-type glassware on a dual manifold Schlenk line, or interfaced to a high-vacuum ($10^{-5}$ Torr) line, or in a nitrogen-filled Vacuum Atmospheres glovebox with a high-capacity recirculator (<2 ppm $O_2$). Argon (Matheson, prepurified), hydrogen (Linde), and deuterium (Isotec) were purified by passage through a MnO oxygen-removal column[30] and a Davison 4 Å molecular sieve column. High-pressure hydrogenation reactions were performed under UHP-grade hydrogen (Linde), used without further purification. Hydrogen for catalytic hydrogenation kinetic studies was additionally purified *via* passage through a freshly activated column of MnO/silica[30] positioned immediately before the reaction vessel. Ether solvents were distilled under nitrogen from sodium benzophenone ketyl. Hydrocarbon solvents (toluene, pentane, heptane) were distilled under nitrogen from Na/K alloy. All solvents for vacuum line manipulations were stored in vacuo over Na/K alloy in resealable bulbs. Deuterated solvents for NMR measurements were obtained from Cambridge Isotope Laboratories (all 99+ atom % D) and were degassed, dried, and stored *in vacuo* over Na/K alloy prior to use. Heptane and diethyl ether (Aldrich, HPLC grade) for circular dichroism spectroscopy were degassed, dried over Na/K alloy, and vacuum-transferred immediately before sample preparation.

The prochiral olefins 2-phenyl-1-butene and 2-ethyl-1-hexene (prepared from propiophenone and heptan-3-one, respectively, *via* Wittig reaction with (methylene)triphenylphosphorane[31]) and 1-pentene (Aldrich) were degassed, dried over Na/K alloy for 0.5 h, and vacuum transferred prior to use. Styrene (Aldrich, Gold Label) was washed with base, distilled twice from $CaH_2$, and vacuum transferred from $CaH_2$ immediately prior to use. The diolefin 1,6-heptadien-4-ol (Wiley) was converted to the *tert*-butyldimethylsilyl ether by standard methods.[32] All diolefin substrates, including 1,5-hexadiene

(27) Stern, D.; Sabat, M.; Marks, T. J. *J. Am. Chem. Soc.* **1990**, *112*, 9558−9575.

(28) Nomenclature in the present case is a straightforward extension of the protocol delineated by Sloan and others and modified to describe previously reported $Me_2SiCp''(R^*Cp)$ complexes.[26a] In this procedure, one views the Cp ring of interest along the vector from the metal to the ring centroid and then ranks the ring substituents according to their Cahn−Ingold−Prelog (CIP) priorities. The direction of travel from highest to lowest priority substituents on the Cp ring will be either clockwise or anticlockwise, and the corresponding designation either *R* or *S*, respectively. Epimeric mixtures, i.e., 50:50 mixtures of *R* and *S* diastereomers, are given the designation *R*/*S*. Because the $Me_3SiCp$ moiety has the higher CIP priority, both its stereochemical designation and its structural formula are indicated first. Thus **9**−**12** in Scheme 1 depict the (*S*,*R*), (*R*,*S*), (*S*,*S*), and (*R*,*R*) configurations of the $Me_2Si(Me_3Si)Cp[(-)$-menthyl$]CpLn$ template, respectively. See also: (a) Sloan, T. E. *Top. Stereochem.* **1981**, *12*, 1−36. (b) Stanley, K.; Baird, M. C. *J. Am. Chem. Soc.* **1975**, *97*, 6598−6599. (c) Krow, G. *Top. Stereochem.* **1970**, *5*, 31−68.

(29) Schaverien, C. J. *Organometallics* **1994**, *13*, 69−82.

(30) (a) He, M.-Y.; Xiong, G.; Toscano, P. J.; Burwell, R. L., Jr.; Marks, T. J. *J. Am. Chem. Soc.* **1985**, *107*, 641−652. (b) Moeseler, R.; Horvath, B.; Lindenau, D.; Horvath, E. G.; Krauss, H. L. *Z. Naturforsch., B* **1976**, *31B*, 892−893. (c) McIlwrick, C. R.; Phillips, C. S. G.; *J. Chem. Phys. E* **1973**, *6*, 1208−1210.

(31) (a) Maryanoff, B. E.; Reitz, A. B. *Chem. Rev.* **1989**, *89*, 863−927. (b) Maecker, A. *Org. React.* **1965**, *14*, 270.

(32) Greene, T. W.; Wuts, P. G. M. *Protective Groups in Organic Synthesis*, 2nd ed.; Wiley: New York, 1991.

Downloaded by CARLI CONSORTIUM on June 30, 2009
Published on April 2, 1996 on http://pubs.acs.org | doi: 10.1021/om950871v

Downloaded by CARLI CONSORTIUM on June 30, 2009
Published on April 2, 1996 on http://pubs.acs.org | doi: 10.1021/om950871v

(Aldrich) and 2-methyl-1,5-hexadiene (Wiley), were twice distilled from $CaH_2$, degassed, and vacuum transferred from Na/K alloy before use.

Anhydrous lanthanide trichlorides were prepared from the corresponding sesquioxides $Ln_2O_3$ (Cerac, Ln = Sm, Y, Lu) and ammonium chloride.[33] Sodium (−)-menthylcyclopentadienide (Na[(−)-menthylCp]),[26a] 1-(chlorodimethylsilyl)-1-(trimethylsilyl)cyclopentadiene,[34] and the solid lithium reagents $LiCH_2SiMe_3$[35] and $LiCH(SiMe_3)_2$[36] were prepared according to published methods.

**Physical and Analytical Measurements.** NMR spectra were recorded on either a Varian Gemini 300 (FT, 300 MHz, $^1$H; 75 MHz, $^{13}$C) or a Varian XL-400 (FT, 400 MHz, $^1$H; 100 MHz, $^{13}$C) instrument. Chemical shifts for $^1$H and $^{13}$C NMR are referenced to internal solvent resonances and are reported relative to tetramethylsilane. NMR experiments on air-sensitive samples were conducted in either Teflon valve-sealed tubes (J. Young) or in screw-capped tubes fitted with septa (Wilmad). Optical rotations were measured at 25 °C with an Optical Activity Ltd. AA-100 polarimeter (±0.001°) using 0.5 dm (2-phenylbutane) and 0.1 dm (neat chiral hydrocarbon products) quartz cells. Concentrations reported with specific rotations are in units of g·(100 cm$^2$)$^{-1}$. Analytical gas chromatography was performed on a Hewlett-Packard 5580A instrument interfaced to a digital recorder/integrator and using a 0.125 inch i.d., 3.8% w/w SE-30 liquid phase on Chromosorb W column. Gas chromatography/ electron impact mass spectra were obtained using a Hewlett Packard 5890 GC interfaced to a VG-70-250 SE spectrometer. A 15 M narrow bore J + W Scientific DB-1 fused silica capillary with 1.0 $\mu$m film thickness was employed as the column material. An ion source potential of 70 eV and inlet source temperature of 200 °C, and a column temperature ramp rate of 10 °C/ min from ambient to 200 °C, were used in GC/MS experiments. All mass spectra were calibrated using PCR perfluorokerosene 755. Circular dichroism spectra were recorded on a Jasco J-500 spectrophotometer equipped with a Jasco DP-500/AT software package (Version 1.2). Air-sensitive samples were prepared in 1 mm or 10 mm path length cylindrical quartz cuvettes (Hellma Cells) modified with Teflon needle valves. Solvent blanks were recorded under identical conditions and the baseline subtracted from the experimental spectrum. Molecular ellipticities [$\theta$] are reported relative to absorption maxima in units of deg·cm$^2$·decimol$^{-1}$. Elemental analyses were performed by Oneida Research Services, Inc., Whitesboro, New York.

**$Li_2Me_2Si(Me_3SiCp)$[(−)-menthylCp] (1).** A 250 mL flask with a Teflon inlet valve was charged with Na[(−)-menthylCp] (12.03 g, 53.15 mmol) in the glovebox. The flask was then transferred to a vacuum line, and THF (150 mL) was added *via* syringe. The mixture was stirred, completely dissolving the solids and affording a clear, amber solution. Under an argon flush, $Me_2Si(Me_3SiCp)Cl$ (12.1 g, 52.4 mmol) was slowly syringed into the stirred solution of the sodium salt. As the addition progressed, the solution began to take on an opalescent appearance, the precipitated NaCl eventually rendering the solution completely opaque. The suspension was stirred at ambient temperature for 10 h. The solvent was then removed *in vacuo*, and pentane (150 mL) was added to the reaction flask to facilitate the precipitation of NaCl. The pentane was removed *in vacuo* and the opaque, gummy liquid exposed to vacuum for ∼3 h. A further aliquot of pentane (150 mL) was added to dissolve the crude ligand. The resulting mixture was filtered and the colorless precipitate washed once with pentane (30 mL). A solution of $LiCH_2SiMe_3$ (9.37 g, 99.6 mmol) in pentane (50 mL) was added slowly from a 100 mL side arm flask to the stirred solution of $Me_2Si(Me_3SiCpH)$[(−)-menthylCpH]. The rate of addition was adjusted to moderate the evolution of gaseous $SiMe_4$ from the exothermic reaction. After the solution was stirred for 8 h, the solvent was removed *in vacuo*. Total isolated yield of $Li_2Me_2Si(Me_3SiCp)$[(−)-menthylCp]: 20.4 g (95%) as a colorless, solvent-free, foamy solid.

Solutions of **1** are prone to gelation as they become more concentrated during solvent removal. The addition of small amounts of THF (5−10 mL) effectively disperses the gel and assists solvent removal. The solid product can be washed with but not recrystallized from pentane. Proton NMR indicates the presence of approximately 1 equiv of THF per ligand molecule. Use of this adduct, **1**·THF, for subsequent reaction with lanthanide(III) halides gives results identical to those with **1**.

$^1$H NMR (THF-$d_8$): $\delta$ 6.40 (m, 1H), 6.37 (m, 1H), 6.23 (m, 1H), 6.10 (m, 1H), 6.00 (m, 1H), 5.84 (m, 1H), 2.44 (m, 1H), 1.95 (m, 1 H), 1.77 (m, 1 H), 1.73 (m, 1 H), 1.68 (m, 1 H), 1.40 (br m, 1 H), 1.35−1.19 (m, 2 H), 1.10 (m, 1 H), 0.99 (m, 1 H), 0.86 (d, 3 H), 0.78 (d, 3 H), 0.75 (d, 3 H), 0.46 (s, 6 H), 0.23 (s, 9 H). $^{13}$C{$^1$H} NMR (THF-$d_8$): $\delta$ 119.2, 117.5, 114.6, 113.6, 111.9, 110.4, 109.7, 104.3, 67.9, 50.1, 48.3, 43.6, 36.3, 34.2, 27.5, 25.8, 25.5, 23.2, 22.0, 16.0, 2.3, 1.6.

**(*S*,*R*)-$Me_2Si(Me_3SiCp)$[(−)-menthylCp]Y($\mu$-Cl)$_2$Li(OEt$_2$)$_2$ (2a).** A 100 mL flask with a Teflon inlet valve was charged with $YCl_3$ (1.77 g, 9.06 mmol) and **1** (3.36 g, 8.18 mmol). THF (80 mL) was condensed into the reaction flask *in vacuo* at −78 °C. All solids dissolved as the solution warmed to room temperature, and the pale yellow, slightly opaque reaction mixture was stirred for 12 h at ambient temperature under argon. Next, the solvent was removed *in vacuo*, and the resulting colorless, gummy solid was dried under high vacuum for 2 h. Diethyl ether (50 mL) was then condensed into the reaction flask *in vacuo* at −78 °C. The solid was triturated several times with diethyl ether at room temperature, and the resulting mixture was filtered. The clear, amber filtrate was evaporated to yield a gummy, colorless solid, which was exchanged repetitively with diethyl ether (30 mL) until a colorless solid precipitated upon solvent removal. Usually 5−6 repetitions were necessary. Alternatively, the diethyl ether solution could be stirred for extended periods (1−2 days) rather than repetitively triturated. This approach is equally effective and requires less solvent. In either case, the resulting solid was then dissolved in a minimum of diethyl ether and the solution slowly cooled to −78 °C. The colorless to pale-yellow crystals of (*S*,*R*)-$Me_2Si(Me_3SiCp)$[(−)-menthylCp]Y($\mu$-Cl)$_2$Li(OEt$_2$)$_2$ were isolated by decanting the mother liquor and vacuum-drying. Additional crops of product could be recovered in a similar fashion from the mother liquor. Total yield: 1.86 g (35%). The product can be additionally recrystallized from cold (−78 °C) diethyl ether to afford colorless blocks of analytically pure **2a**.

$^1$H NMR (THF-$d_8$, −20 °C): $\delta$ 6.18 (m, 1H), 6.05 (m, 2 H), 5.81 (m, 1 H), 5.77 (m, 1 H), 5.76 (m, 1 H), 3.37 (q, 8 H), 2.43 (m, 1 H), 1.78 (m, 1 H), 1.76−1.67 (m, 2 H), 1.62 (m, 1 H), 1.38 (br m, 1 H), 1.13 (t, 12 H), 1.06 (m, 1 H), 1.03 (m, 1 H), 0.89 (d, 3 H), 0.89−0.77 (m, 2 H), 0.77 (d, 3 H), 0.72 (d, 3 H), 0.62 (s, 3 H), 0.50 (s, 3 H), 0.17 (s, 9 H). $^{13}$C{$^1$H} NMR (THF-$d_8$, −20 °C): $\delta$ 139.7, 128.7, 120.9, 120.1, 117.9, 117.0, 115.9, 115.0, 111.7, 109.1, 66.4, 51.3, 42.7, 41.5, 36.7, 34.1, 27.5, 23.3, 22.2, 16.3, 15.8, 0.4, −2.6, −4.6. CD (Et$_2$O, 25 °C), $\lambda_{max}$ ([$\theta$]): 301 (−4440), 273 sh (−8160), 261 (−12 670) nm. Anal. Calcd for $C_{33}H_{60}Cl_2LiO_2Si_2Y$: C, 55.69; H, 8.50; Cl, 9.96. Found: C, 55.55; H, 8.47; Cl, 10.00.

**(*S*,*R*)-$Me_2Si(Me_3SiCp)$[(−)-menthylCp]Lu($\mu$-Cl)$_2$Li(OEt$_2$)$_2$ (2b).** The procedure detailed above for the yttrium analog was used with $LuCl_3$ (3.40 g, 12.1 mmol) and $Li_2Me_2Si(Me_3SiCp)$[(−)-menthylCp] (4.00 g, 10.1 mmol) in THF (80 mL). The total yield of (*S*,*R*)-$Me_2Si(Me_3SiCp)$[(−)-menthylCp]-Lu($\mu$-Cl)$_2$Li(OEt$_2$)$_2$ was 4.3 g (54%), isolated as colorless crystals.

(33) Meyer, G. *Inorg. Synth.* **1989**, *25*, 146−150.
(34) Rozell, J. M., Jr.; Jones, P. R. *Organometallics* **1985**, *4*, 2206−2210
(35) Tessier-Youngs, C.; Beachley, O. T., Jr. *Inorg. Synth.* **1986**, *24*, 95−97.
(36) Cowley, A. H.; Kemp, R. A. *Synth. React. Inorg. Met.-Org. Chem.* **1981**, *11*, 591−595.

Downloaded by CARLI CONSORTIUM on June 30, 2009
Published on April 2, 1996 on http://pubs.acs.org | doi: 10.1021/om950871v

$^1$H NMR (THF-$d_8$, −20 °C): $\delta$ 6.10 (m, 1 H), 6.00 (m, 1 H), 5.96 (m, 1 H), 5.70−5.73 (m, 2 H), 5.68 (m, 1 H), 3.38 (q, 8 H), 2.43 (m, 1 H), 1.85−1.65 (m, 3 H), 1.62 (m, 1 H), 1.38 (m, 1 H), 1.13 (t, 12 H), 1.1−0.96 (m, 3 H), 0.89 (d, 3 H), 0.88 (m, 1 H), 0.83 (m, 1 H), 0.77 (d, 3 H), 0.71 (d, 3 H), 0.60 (s, 3 H), 0.48 (s, 3 H), 0.16 (s, 9 H). CD ($Et_2O$, 25 °C), $\lambda_{max}$ ([$\theta$]): 291 (−5010), 267 sh (−6890), 254 (−11 970) nm. Anal. Calcd for $C_{33}H_{60}Cl_2LiLuO_2Si_2$: C, 49.68; H, 7.58; Cl, 8.89. Found: C, 49.56; H, 7.56; Cl, 8.92.

**(*S*,*R*)-Me$_2$Si(Me$_3$SiCp)[(−)-menthylCp]YCH(SiMe$_3$)$_2$ (3a).** A 50 mL flask was charged with (*S*,*R*)-Me$_2$Si(Me$_3$SiCp)[(−)-menthylCp]Y($\mu$-Cl)$_2$Li(OEt$_2$)$_2$ (0.47 g, 0.66 mmol) and LiCH(SiMe$_3$)$_2$ (0.11 g, 0.66 mmol). Toluene (30 mL) was condensed into the reaction flask *in vacuo* at −78 °C. After backfilling with argon, the mixture was placed in an ice/water bath (−5 °C). The reaction was allowed to warm slowly to room temperature with stirring over 12 h. The solvent was then removed *in vacuo* and the resulting colorless oil was dried under high vacuum for 2 h. Pentane (25 mL) was then condensed into the flask *in vacuo*, at −78 °C. Upon warming, the solvent was removed and the trituration repeated four times. Careful and occasionally multiple filtrations were required to ensure complete removal of lithium chloride. Evaporation of solvent *in vacuo* gave the alkyl derivative in essentially quantitative yield (0.40 g, 95% yield) as a colorless to pale-yellow powder. No LiCH(SiMe$_3$)$_2$ was detected in the $^1$H NMR, and the solid was determined to be analytically pure.

$^1$H NMR (toluene-$d_8$, 100 °C): $\delta$ 6.78 (br s, 1 H), 6.57−6.40 (br m, 2 H), 6.25 (br s, 1 H), 6.18 (br s, 1 H), 5.95 (br s, 1 H), 2.31 (m, 1 H), 1.70 (m, 1 H), 1.66−1.54 (m, 2 H), 1.40−1.20 (m, 3 H), 1.06−0.84 (m, 3 H), 0.91 (d, 3 H), 0.77 (d, 3 H), 0.73 (s, 3 H), 0.70 (d, 3 H), 0.53 (s, 3 H), 0.15 (s, 18 H), 0.14 (s, 9 H). CD (*n*-heptane, 25 °C), $\lambda_{max}$ ([$\theta$]): 312 (−8720), 281 (−18 530) nm. Anal. Calcd for $C_{32}H_{59}Si_4Y$: C, 59.58; H, 9.22. Found: C, 59.45; H, 9.07.

**(*S*,*R*)-Me$_2$Si(Me$_3$SiCp)[(−)-menthylCp]LuCH(SiMe$_3$)$_2$ (3b).** The procedure detailed above for the yttrium analog was used with (*S*,*R*)-Me$_2$Si(Me$_3$SiCp)[(−)-menthylCp]Lu($\mu$-Cl)$_2$Li(OEt$_2$)$_2$ (1.00 g, 1.25 mmol) and LiCH(SiMe$_3$)$_2$ (0.208 g, 1.25 mmol) in toluene (30 mL). Isolated yield of **3b**: 0.87 g (95% yield) as a colorless powder.

$^1$H NMR (toluene-$d_8$, 25 °C): $\delta$ 6.92 (m), 6.66 (m), 6.62 (m), 6.53 (m), 6.50 (m), 6.38 (m), 6.29 (m), 6.24 (m), 6.19 (m), 6.16 (m), 6.05 (m), 5.91 (m), 2.24 (m), 1.72 (m), 1.61 (m), 1.31 (m), 0.98 (d), 0.93 (m), 0.84 (d), 0.78 (d), 0.75 (s), 0.72 (d), 0.71 (d), 0.53 (s), 0.35 (s), 0.34 (s), 0.31 (d), 0.16 (s), 0.15 (s), 0.13 (s). $^{13}$C{$^1$H} NMR (toluene-$d_8$, 25 °C): $\delta$ 140.1, 139.4, 129.8, 129.8, 127.4, 127.2, 125.2, 122.5, 121.6, 121.5, 120.4, 118.9, 118.3, 117.7, 116.8, 114.5, 112.7, 112.6, 111.9, 109.9, 51.7, 51.6, 42.4, 42.2, 41.6, 41.5, 35.5, 33.5, 28.5, 28.3, 27.3, 25.0, 22.7, 21.7, 21.6, 15.8, 15.6, 5.3, 5.2, 2.7, 2.3, 2.1, 1.4, 0.4, 0.3, 0.2, 0.0, −2.2, −2.5, −5.7. CD (*n*-heptane, 25 °C), $\lambda_{max}$ ([$\theta$]): 304 (-8160), 271 (−13 290) nm. Anal. Calcd for $C_{32}H_{59}LuSi_4$: C, 52.57; H, 8.13. Found: C, 52.43; H, 8.09.

**X-ray Crystallographic Study of (*S*,*R*)-Me$_2$Si(Me$_3$SiCp)[(−)-menthylCp]Lu($\mu$-Cl)$_2$Li(OEt$_2$)$_2$ (2b).** The transparent, colorless crystal of **2b** used for data collection had rounded faces and edges. The crystal was cut from a larger crystal and mounted using oil (Paratone-N, Exxon) on a thin glass fiber and then cooled to −120 °C on an Enraf-Nonius CAD4 automated $\kappa$-axis diffractometer. The crystal, data collection, and refinement parameters are collected in Table 1. Corrections for Lorentz and polarization effects[37] and anomalous dispersion effects[37b,38] were applied to the data as was a numerical absorption correction.[37c,38a,39]

**Table 1. Crystallographic Details for (*S*,*R*)-Me$_2$Si(Me$_3$SiCp)[(−)-menthylCp]Lu($\mu$-Cl)$_2$Li(OEt$_2$)$_2$ (2b)**

| | |
|---|---|
| formula | $LuCl_2Si_2O_2C_{33}LiH_{60}$ |
| fw | 797.832 |
| cryst color, habit | colorless blocks |
| Cryst dimens, mm | 0.3 × 0.3 × 0.5 |
| cryst system | triclinic |
| *a*, Å | 11.580(4) |
| *b*, Å | 11.756(2) |
| *c*, Å | 16.678(4) |
| $\alpha$, deg | 108.93(2) |
| $\beta$, deg | 94.52(2) |
| $\gamma$, deg | 110.50(2) |
| *V*, Å$^3$ | 1964(1) |
| space group | *P*1 |
| Z | 2 |
| *d*(calc), g/cm$^3$ | 1.339 |
| diffractometer | Enraf-Nonius CAD4 |
| temp °C | −120 °C |
| transm factors range | 0.431−0.546 (numerical) |
| radiation | Mo, $\lambda$(K$\alpha$) = 0.710 73 Å, graphite monochromator |
| scan Type | $\omega/\theta$ |
| 2$\theta$ range, deg | 2.0−45.0 ($\pm h$, $\pm k$, $\pm l$) |
| intensities (unique, $R_i$) | 10 908 |
| intensities > 2.58$\sigma$(*I*) | 10 122 |
| *R* | 0.040 |
| $R_w$ for $w = 1/s^2(F_0)$ | 0.051 |

The structure was solved by Patterson methods (SHELXs-86),[37e,40] and the correct Lu positions were deduced from a vector map. Subsequent least-squares-difference Fourier calculations revealed atomic positions for the remaining non-hydrogen atoms. Hydrogen atoms were included as fixed contributors in "idealized" positions. In the final cycle of least-squares refinement, isotropic thermal coefficients were refined for both carbon and lithium atoms. A disorder principally affecting atoms C(26) and C(27) of the ether molecule could not be consistently modeled. Isotropic thermal coefficients were refined for the carbon and lithium atoms, and anisotropic thermal coefficients, for the remaining non-hydrogen atoms. Group isotropic thermal parameters were refined for the hydrogen atoms, and an isotropic extinction parameter was varied. The highest peaks remaining in the final difference Fourier map were in the vicinity of Lu atoms. A final analysis of variance between observed and calculated structure factors showed no apparent systematic error. Absolute configuration followed from the known configuration of the chiral auxiliary. All computer programs and the sources of the scattering factors are contained in the SHELXTL program library (5.1) (G. Sheldrick, Nicolet Corp., Madison, WI).

**NMR-Scale Reaction of Hydrocarbyl Precatalysts with Hydrogen.** In the glovebox, an NMR tube fitted with a Teflon valve was loaded with (*S*,*R*)-Me$_2$Si(Me$_3$SiCp)[(−)-menthylCp]LnCH(SiMe$_3$)$_2$ (5−10 mg, ∼0.015 mmol). The tube was sealed, transported outside, and interfaced to the vacuum line. Cyclohexane-$d_{12}$ or methylcyclohexane-$d_{14}$ (∼0.5 mL) was vacuum transferred at −78 °C onto the sample. The tube was then backfilled with $H_2$ (1 atm) and sealed while the entire tube was maintained at −78 °C (resulting in a final hydrogen pressure of ∼1.5 atm at room temperature). The sample was then inserted into the NMR probe at room temperature.

(37) Stout, G. H.; Jensen, J. H. *X-Ray Structure Determination, a Practical Guide*; Macmillan: New York, 1968; and references therein: (a) Lorentz and polarization, pp 195−200. (b) Anomalous dispersion, pp 234−237. (c) Absorption, pp 204−205. (d) Extinction, pp. 409−412. (e) Patterson function; see Fourier synthesis and pp 270−288. (f) Direct methods, pp 315−338. (g) Vector methods, pp 339−349. (h) Fourier synthesis, pp 222−226, 246−262, 353−362, 381, 445−448. (i) Least squares, pp 385−394, 395−397, 405−406, 454−458. (j) Structure factors, pp 217−222, 230−246, 262.

(38) *International Tables for X-Ray Crystallography*; Ibers, J. A., Hamilton, W. C., Eds.; Kynoch Press: Birmingham, 1974; Vol. IV: (a) Mass attenuation coefficients, pp 61−66. (b) Analytical approximation to the scattering factors, pp 99−101. (c) Anomalous dispersion corrections, pp 149−150.

(39) The crystal was assumed to be a convex polyhedron bound by plane surfaces, i.e., the crystal faces. A numerical integration of the beam path length was carried out over the entire volume of the sample to evaluate the transmission coefficient for each reflection. For a complete description see: Busing, W. R.; Levy, H. A. *Acta Crystallogr.* **1957**, *10*, 180.

(40) Calculations were performed on a DEC VAX 11/750 computer system.

Downloaded by CARLI CONSORTIUM on June 30, 2009
Published on April 2, 1996 on http://pubs.acs.org | doi: 10.1021/om950871v

Reaction was evident almost immediately, indicated by the appearance of $CH_2(SiMe_3)_2$ in the $^1H$ NMR spectrum. The reaction was allowed to proceed at room temperature for 24 h with constant mixing, NMR monitoring, and the addition of $H_2$ as necessary to ensure that the final "$t = \infty$" spectrum contained a visible excess of $H_2$. The NMR spectrum of the resulting sample was then recorded over the range −80 to 100 °C.

**Preparative-Scale Olefin Hydrogenation and Reductive Cyclization of α,ω-Diolefins.** In the glovebox, a 20 mL flamed cylindrical Pyrex reaction vessel, equipped with a Teflon inlet valve and a magnetic stir bar, was charged with the (*S*,*R*)-$Me_2Si(Me_3SiCp)$[(−)-menthylCp]LnCH$(SiMe_3)_2$ precatalyst (10−20 mg, ∼0.03 mmol). On the vacuum line, pentane (0−3.0 mL) was condensed into the reaction apparatus *in vacuo* at −78°C followed by the olefin or diolefin (0.5−1.0 mL, ∼3.0−6.0 mmol). The vessel was backfilled with $H_2$ or $D_2$ and warmed to ambient temperature (22 ± 1°C) with vigorous stirring. Consumption of $H_2$ was monitored by mercury manometer. During reductions of the styrenic substrates, the reaction mixtures took on a yellowish tint which then slowly faded as the rate of hydrogen uptake slowed toward the end of the reaction. After $H_2$ uptake had ceased, the volatiles were vacuum transferred from the reaction mixture and the pentane removed by rotary evaporation, if necessary. Product purity was determined by $^1H$ NMR, GC, and GC/MS, and product enantiomeric excess was determined by comparison to known rotations.[41]

**Kinetics of Catalytic Enantioselective Olefin Hydrogenation.** Kinetic studies were performed in the all glass, metal, and Teflon grease-free, constant-volume, pseudo-constant-pressure, gas-uptake apparatus described previously.[16a] In a typical experiment, the oven-dried, jacketed reactor was attached to the vacuum line while still hot, evacuated/backfilled with argon 5−7 times, and finally evacuated continuously for at least 1 h (ultimate vacuum attainable, (2−4) × $10^{-6}$ Torr). The burets were then backfilled with argon and sealed, and the entire reaction vessel was transported into the glovebox. The burets were then filled with freshly-prepared, volumetric solutions of (*S*,*R*)-$Me_2Si(Me_3SiCp)$[(−)-menthylCp]-YCH$(SiMe_3)_2$ (2−20 mM) and 2-phenyl-1-butene in *n*-heptane (0.950 or 1.90 M). The burets were tightly sealed, and the entire apparatus was quickly transported outside to the vacuum line. The reaction volume was evacuated/backfilled with argon (more efficient displacement of air and moisture) until the ultimate vacuum was < 2 × $10^{-6}$ Torr. The apparatus was subsequently evacuated/backfilled with $H_2$ repetitively—usually 5−6 times—to ensure complete removal of argon. On the ultimate evacuation cycle, the pressure was recorded from a mercury manometer. The entire system was then filled with $H_2$ and adjusted to the desired pressure. A thermostated (±0.2 °C) water circulating system was connected to the reactor jacket and actuated. After all components had attained thermal equilibrium and equilibrium with the reactor atmosphere, a measured volume of olefin solution (1.00 mL) was titrated into the reactor. (For the preparative-scale reaction under non-mass-transport limited conditions, ∼0.5 mL of neat olefin was used at 700 Torr $H_2$ pressure.) Stirring (vortex agitation) was then initiated to equilibrate the atmosphere with solvent vapor, and a final pressure reading was recorded from the manometer. A measured aliquot of the catalyst solution (1.00 mL) was quickly transferred to the reaction vessel, and the change in $H_2$ pressure was recorded as a function of time using the previously described electronic manometer.[16a] As each trial progressed, a noticeable yellowing of the reaction mixture could be observed, although the solutions remained clear. Initial apprehensions with respect to contamination or poisoning of the catalytic system proved baseless, however, as the reaction mixtures returned to their original colorless appearance at the conclusion of $H_2$ uptake, yielding the product alkane quantitatively (by $^1H$ NMR) upon workup. Conditions were adjusted such that, for all lanthanide (∼1−10 mM) and olefin (∼0.5−2 M) concentrations, the overall drop in $H_2$ pressure was always less than 2% (usually <1%) of its initial value (180−700 Torr). The instantaneous reaction rate ($v$) at a particular substrate concentration ($C$) was estimated at a number of points over at least a 10-fold range of $C$ by fitting the data on a small segment of the uptake curve (essentially the instantaneous slope) *via* least-squares analysis to eq 1, where $C_1 = C + x$

$$C_1 - C_2 = vt \tag{1}$$

$$N_t\ (s^{-1}) = v/[Ln]_T \tag{2}$$

and $C_2 = C - x$ are the olefin concentrations at the start and end of the assay, respectively. The interval of each assay (i.e., $2x$) was always less than $0.3C_1$ and usually ∼$0.05C_1$.[42] The turnover frequency ($N_t$) was thus estimated for a given catalyst concentration and hydrogen pressure by eq 2, where $[Ln]_T$ is the total concentration of the catalyst precursor.

## Results

The synthesis of the chiral chelating ligand $Me_2Si(3\text{-}Me_3SiCp)[3\text{-}(-)\text{-menthylCp}]^{2-}$ (**1**) will be discussed briefly, followed by the synthesis and characterization of the chiral organolanthanide chloro complexes. Attention will be paid to structural characterization by spectroscopic techniques and X-ray diffraction. The preparation of the chiral hydrocarbyl catalyst precursors then follows, along with an examination of the solution structural dynamic behavior. The reactivity of the organolanthanide hydrocarbyls with hydrogen—alone and in the presence of olefinic substrates—is presented next, along with kinetic/mechanistic studies of the catalytic asymmetric hydrogenation of 2-phenyl-1-butene by (*S*,*R*)-$Me_2Si(Me_3SiCp)$[(−)-menthylCp]Y−R. These reactions will be examined in light of structure/reactivity patterns observed with previously studied organolanthanide catalysts,[15b,26,27] especially as they relate to the degree of coordinative unsaturation. Previous work showed that while $Me_2SiCp''(R^*Cp)LnR$ catalysts were highly efficient for the hydrogenation or deuteration of styrene-based olefins, similar asymmetric reductions of simple olefins such as 1-pentene were not as successful (low turnover capacity), presumably due to competitive β-hydrogen elimination. The present class of complexes, by virtue of the increased hardness/decreased electron-donating capacity of $Me_3SiCp$ *vs.* Cp″, might be expected to eschew such a pathway.[29,43] The origins of enantioselectivity in the hydrogenation reaction will also be analyzed on the basis of catalyst−substrate steric interactions.

**Ligand Synthesis.** The synthesis of chiral chelating ligand **1** is shown in Scheme 2. Coupling of Na[(−)-

(41) (a) Elsenbaumer, R. L; Mosher, H. S. *J. Org. Chem.* **1979**, *44*, 600−604. (b) Lardicci, L.; Menicagli, R.; Salvadori, *P. Gazz. Chim. Ital.* **1968**, *98*, 738−759. (c) Streitwieser, A.; Granger, M. R. *J. Org. Chem.* **1967**, *32*, 1528−1529.

(42) Lee, H.-J.; Wilson, I. B. *Biochim. Biophys. Acta* **1971**, *242*, 519.

(43) (a) Bruno, J. W.; Marks, T. J.; Morss, L. R. *J. Am. Chem. Soc.* **1993**, *105*, 6824. (b) Nolan, S. P.; Stern, D.; Hedden, D.; Marks, T. J. In *Bonding Energetics in Organometallic Compounds*; Marks, T. J., Ed.; ACS Symposium Series 428; American Chemical Society: Washington, DC, 1990; p 159. (c) Nolan, S. P.; Stern, D.; Marks, T. J. *J. Am. Chem. Soc.* **1989**, *111*, 7844. (d) Ziegler, T.; Tschinke, V.; Versluis, L.; Baerends, E. J.; Ravenek, W. *Polyhedron* **1988**, *7*, 1625. (e) Schock, L. E.; Marks, T. J. *J. Am. Chem. Soc.* **1988**, *110*, 7701. (f) Lin, Z.; Marks, T. J. *J. Am. Chem. Soc.* **1987**, *109*, 7979. (g) Bruno, J. W.; Stecher, H. A.; Morss, L. R.; Sonnenberger, D. C.; Marks, T. J. *J. Am. Chem. Soc.* **1986**, *108*, 7275. (h) Sonnenberger, D. C.; Morss, L. R.; Marks, T. J. *Organometallics* **1985**, *4*, 352.

**Scheme 2. Synthesis of the Chiral Chelating Ligand Reagent $Me_2Si(Me_3SiCp)[(-)$-menthylCp$]Li_2$ (1)**

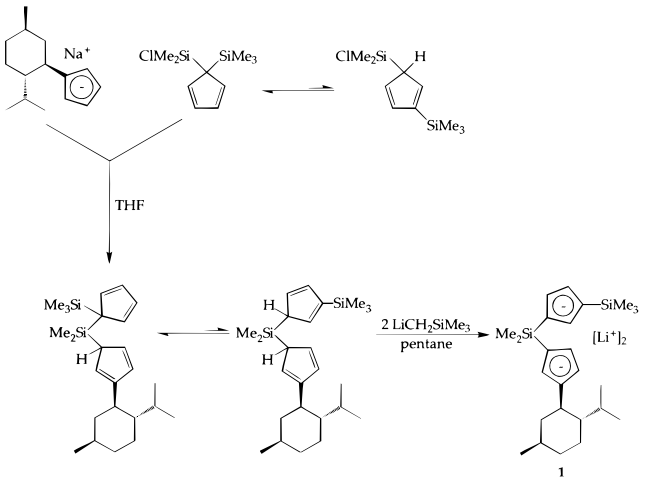


menthylCp] with 1-(chlorodimethylsilyl)-1-(trimethylsilyl)cyclopentadiene in THF yields the neutral ligand which is then cleanly converted to dilithium salt **1** by reaction with 2 equiv of $LiCH_2SiMe_3$ in pentane. Addition of a small amount of THF to pentane solutions of **1** aids in the removal of solvent and affords an approximately 1:1 (by $^1$H NMR) adduct of the dilithium salt, **1**·THF, as colorless microcrystals, virtually insoluble in pentane. A similar THF solvate of the related ligand $Me_2Si(^t$BuCp$)[(+)$-neomenthylCp$]Li_2$ has also recently been isolated in this manner.[44]

**Chiral Organolanthanide Chloro Precursors.** Transmetalation of **1** with a slight excess of anhydrous yttrium or lutetium trichloride in THF (eq 3), followed

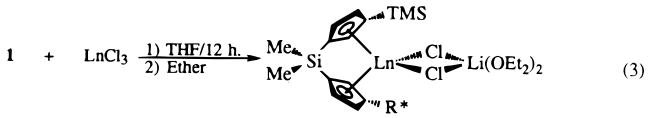


(3)

**2a** Ln = Y
**b** Ln = Lu

by workup in diethyl ether, yields the corresponding chiral lanthanide chloro complexes **2** as analytically pure crystalline solids, typically in ~40% isolated yield. Attempts to synthesize the analogous complexes with larger lanthanides (e.g., neodymium(III), samarium(III)) were unsuccessful, presumably due to their instability with respect to loss of lithium chloride and the formation of insoluble chloro-bridged dimers or oligomers.[13a,b,15]

$^1$H NMR spectra of **2** indicate that the isolated products are diastereomerically pure complexes. Particularly diagnostic is the presence of six multiplets in the cyclopentadienyl region ($\delta$ 5−7 ppm) of the spectra of **2** (Figure 1). Additionally, only one set of three SiMe singlets (one resonance corresponding to the ring $Me_3$Si protons and one for each of the diastereotopic backbone MeSi protons) and one set of three methyl doublets (one doublet for each of the methyl groups of the chiral auxiliary) are present at higher field. Above −20 °C, these complexes are configurationally unstable in THF and undergo epimerization to yield an equilibrium mixture of two major and one minor diastereomeric products, as evidenced by the appearance of 12

(44) Denninger, U. E.; Marks, T. J. Manuscript in preparation.

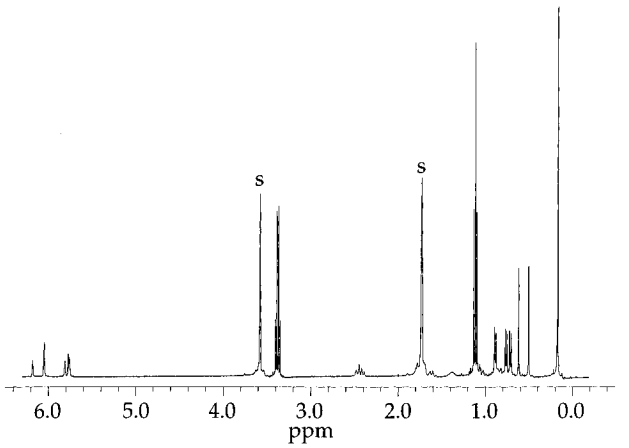


**Figure 1.** $^1$H NMR spectrum (400 MHz) of $Me_2Si(Me_3$SiCp$)[(-)$-menthylCp$]Y(\mu$-Cl$)_2$Li$(OEt_2)_2$ (**2a**) in THF-$d_8$ at −20 °C. S indicates solvent resonances.

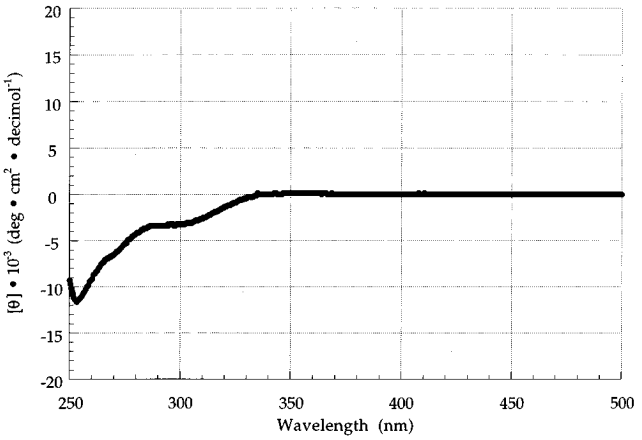


**Figure 2.** Circular dichroism spectrum of $Me_2Si(Me_3$SiCp$)[(-)$-menthylCp$]Lu(\mu$-Cl$)_2$Li$(OEt_2)_2$ (**2b**) in diethyl ether, 25 °C.

additional cyclopentadienyl signals concomitant with a decrease in the intensity of the initial signals attributable to starting material, **2**. Thus, of four possible diastereomers only three are apparent in the NMR at equilibrium in THF-$d_8$. Conversely, in diethyl ether-$d_{10}$, little to no epimerization occurs, and the resonances attributable to **2** (>95% of the cyclopentadienyl signal intensity in the $^1$H NMR spectrum) persist indefinitely.

Circular dichroism spectra of **2** in diethyl ether (Figure 2) display a negative Cotton effect for the major absorptions at 261 nm (**2a**) and 254 nm (**2b**). Previous work established a direct correlation between the sign of the Cotton effect in this spectral region and the attachment mode of R*Cp in $Me_2SiCp''$(R*Cp)Ln$(\mu$-Cl$)_2$Li$(OEt_2)_2$ and $Me_2SiCp''$(R*Cp)LnE$(SiMe_3)_2$ complexes (Ln = Y, Sm, Lu; R* = (+)-neomenthyl, (−)-menthyl; E = CH, N),[26a] as determined by X-ray crystallography: *S* configurations (**15**) give rise to a positive

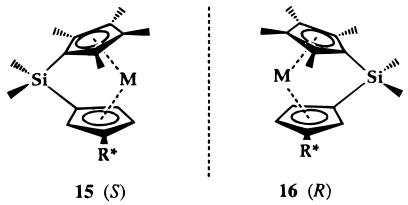


**15** (*S*) **16** (*R*)

Cotton effect, while *R* configurations (**16**) exhibit a

Downloaded by CARLI CONSORTIUM on June 30, 2009
Published on April 2, 1996 on http://pubs.acs.org | doi: 10.1021/om950871v

**Table 2. Selected Bond Lengths (Å) and Angles (deg) in Coordination Groups of (*S,R*)-$Me_2Si$-($Me_3SiCp$)[(−)-menthylCp]Lu($\mu$-Cl)$_2$Li($OEt_2$)$_2$ (2b)[a]**

| | | | |
|---|---|---|---|
| Lu(1)−C(1) | 2.60(1) | Lu(1)−Cl(1) | 2.573(3) |
| Lu(1)−C(2) | 2.56(1) | Lu(1)−Cl(2) | 2.583(2) |
| Lu(1)−C(3) | 2.66(1) | Si(2)−C(3) | 1.86(1) |
| Lu(1)−C(4) | 2.65(1) | C(14)−C(16) | 1.51(1) |
| Lu(1)−C(5) | 2.603(9) | Cl(1)−Li(1) | 2.42(2) |
| Lu(1)−C(11) | 2.554(9) | Cl(2)−Li(1) | 2.39(2) |
| Lu(1)−C(12) | 2.56(1) | O(1)−Li(1) | 1.92(2) |
| Lu(1)−C(13) | 2.57(1) | O(2)−Li(1) | 1.91(2) |
| Lu(1)−C(14) | 2.66(1) | Si(1)−C(1) | 1.88(1) |
| Lu(1)−C(15) | 2.600(10) | Si(1)−C(11) | 1.86(1) |
| Lu(1)−Cg1 | 2.32(1) | Lu(1)−Cg2 | 2.293(9) |
| Cg1−Lu(1)−Cg2 | 122.1(4) | Si(1)−Lu(1)−Li(1) | 159.0(3) |
| C(1)−Si(1)−C(11) | 98.7(5) | C(9)−Si(1)−C(10) | 111.5(6) |
| O(1)−Li(1)−O(2) | 107.9(10) | Cl(1)−Lu(1)−Cl(2) | 86.59(9) |
| Lu(1)−Cl(1)−Li(1) | 89.0(4) | Lu(1)−Cl(2)−Li(1) | 89.3(4) |
| Cl(1)−Li(1)−Cl(2) | 94.4(6) | Lu(1)−C(3)−Si(2) | 129.4(5) |
| Lu(1)−C(14)−C(16) | 127.1(8) | Lu(1)−C(4)−H(4) | 119(1) |
| Lu(1)−C(13)−H(13) | 114.1(10) | | |

[a] Cg = ring centroid.

negative Cotton effect. On the basis of these empirical correlations, which also obtain for the related group 4 $Me_2SiCp''$(R*Cp)$MX_2$ (R* = (+)-neomenthyl, (−)-menthyl; M = Zr, Hf; X = Cl, Me) complexes,[45] it is reasonable to assign the *R* attachment mode to the (−)-menthylCp moiety in **2** from the data in the CD spectra alone. Diffraction data (*vide infra*) confirm this conclusion. The stereochemistry of $Me_3SiCp$ coordination is not readily apparent from either CD or NMR spectra, and unambiguous assignment must rely on X-ray crystallography.

**Molecular Structure of (*S,R*)-$Me_2Si(Me_3SiCp)$-[(−)-menthylCp]Lu($\mu$-Cl)$_2$Li($OEt_2$)$_2$ (2b).** Single-crystal X-ray diffraction analysis of **2b** was used to assign unambiguously the absolute configuration of the complex; data collection parameters and selected bond lengths and angles are given in Tables 1 and 2, respectively. The complex adopts a distorted pseudotetrahedral, bent metallocene motif in which the cyclopentadienyl ring auxiliaries are surprisingly arranged in a structure **9** pseudo-*meso* (*S*, *R*) fashion (Figure 3). The $C_{2v}$ point symmetry found in archetypal $Cp_2LnX_2^-$ complexes[43g,46,47] is lost in **2b**, and the ($\mu$-Cl)$_2$Li($OEt_2$)$_2$ unit is skewed toward the unsubstituted side of the molecule (Figure 3A). This substantial distortion can be quantitatively assessed by the contraction of ∠Si(1)−Lu(1)−Li(1) from a typical[43,46,47] value of ∼180° to 159.0(3)°. The additional observation of close nonbonded contacts between Cl(1) and the trimethylsilyl group (Cl(1)···Si(2) = 3.91 Å) as well as between Cl(1) and C(16) and C(21) (3.66 and 3.70 Å, respectively) of the (−)-menthyl auxiliary implies that, by adopting the

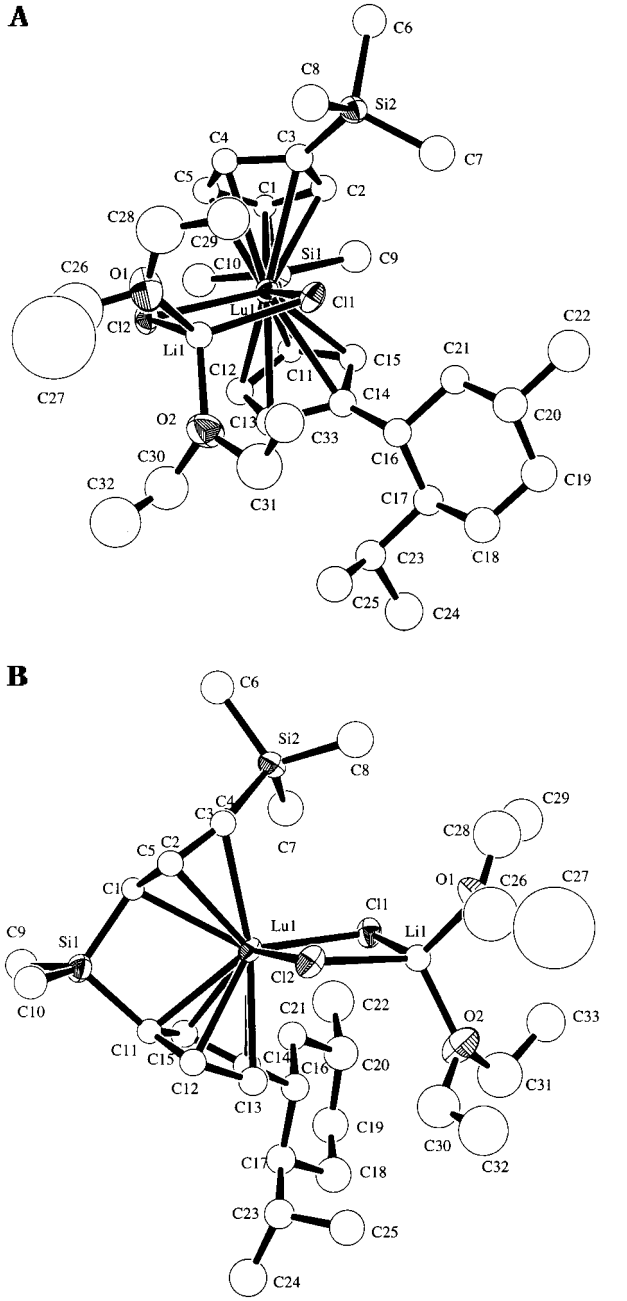


**Figure 3.** Perspective ORTEP views of the molecular structure of (*S,R*)-$Me_2Si(Me_3SiCp)$[(−)-menthylCp]Lu($\mu$-Cl)$_2$Li($OEt_2$)$_2$ (**2b**). Thermal ellipsoids are drawn to encompass 50% probability. (A) View into the "clamshell" showing the skewed bis($\mu$-chloro) bridge, (noncollinear Si(1)−Lu(1)−Li(1)). (B) View of the unsubstituted side of **2b** showing the out-of-plane displacement of the $Li^+$ ion.

observed *meso* configuration, the complex avoids bringing both chloro ligands into repulsive contact with the ring auxiliaries as would likely be the case in *rac* diastereomers (structures **11**, **12**). The crystal structures of various *rac* and *meso* group 4 X(CpR)$_2$MCl$_2$ complexes invite a similar interpretation.[4,10,11,48] Nevertheless, the observation of other isomers upon dissolution in THF suggests other *meso* and *rac* configurations do not differ greatly in free energy and are kinetically accessible.

(45) (a) Giardello, M. A.; Eisen, M. S.; Stern, C. L.; Marks, T. J. *J. Am. Chem. Soc.* **1995**, *117*, 12114−12129. (b) Giardello, M. A.; Eisen, M. S.; Stern, C. L.; Marks, T. J. *J. Am. Chem. Soc.* **1993**, *115*, 3326−3327.

(46) (a) Schumann, H.; Albrecht, I.; Loebel, J.; Hahn, E.; Hossain, M. B.; Van der Helm, D. *Organometallics* **1986**, *5*, 1296−1304. (b) Rausch, M. D.; Moriarty, K. J.; Atwood, J. L.; Weeks, J. A.; Hunter, W. E.; Brittain, H. G. *Organometallics* **1986**, *5*, 1281−1283. (c) Watson, P. L.; Whitney, J. F.; Harlow, R. L. *Inorg. Chem.* **1981**, *20*, 3271−3278. (d) Tilley, T. D.; Andersen, R. A. *Inorg. Chem.* **1981**, *20*, 3267−3271. (e) Wayda, A. L.; Evans, W. E. *Inorg. Chem.* **1980**, *19*, 2190−2191.

(47) (a) Lappert, M. F.; Singh, A.; Atwood, J. L.; Hunter, W. E.; Zhang, H. M. *J. Chem. Soc., Chem. Commun.* **1983**, 69−70. (b) Lappert, M. F.; Singh, A.; Atwood, J. L.; Hunter, W. E. *J. Chem. Soc., Chem. Commun.* **1981**, 1191−1192. (c) Atwood, J. L.; Hunter, W. E.; Rogers, R. D.; Holton, J.; McMeeking, J.; Pearce, R.; Lappert, M. F. *J. Chem. Soc., Chem. Commun.* **1978**, 140−142.

(48) Piemontesi, F.; Camurati, E.; Resconi, L.; Balboni, D.; Sironi, A.; Moret, M.; Ziegler, R.; Piccolrovazzi, N. *Organometallics* **1995**, *14*, 1256.

Downloaded by CARLI CONSORTIUM on June 30, 2009
Published on April 2, 1996 on http://pubs.acs.org | doi: 10.1021/om950871v

Downloaded by CARLI CONSORTIUM on June 30, 2009
Published on April 2, 1996 on http://pubs.acs.org | doi: 10.1021/om950871v

Despite the observed distortion of the Lu coordination geometry in **2b**, there is no gross departure of ∠Cl(1)−Lu(1)−Cl(2) (86.59(9)°) or the Lu−Cl bond lengths (2.573(3) and 2.583(2) Å) from those found in (*R*)-$Me_2$SiCp″[(+)-neomenthylCp]Lu($\mu$-Cl)$_2$Li(OEt$_2$)$_2$[26a] (86.9(1)°; 2.569(4) and 2.571(4) Å) and for achiral Cp′$_2$Yb($\mu$-Cl)$_2$Li(OEt$_2$)$_2$[46] (85.95°; Lu−Cl = 2.586 and 2.584 Å, correcting for differences in $Lu^{3+}$ and $Yb^{3+}$ eight-coordinate ionic radii[49]). The remaining bond distances and angles within the Lu($\mu$-Cl)$_2$Li(OEt$_2$)$_2$ unit of **2b** also compare favorably with the aforementioned structures, with the exception that Li(1) appears to display a small vertical (∼0.07 Å) displacement from the $LuCl_2$ plane (Figure 3B). It is uncertain if this is a result of adventitious packing forces or related to the unusual steric requirements of the ancillary ligation. The latter explanation is perhaps less satisfactory as Li(1) is displaced toward the bulkier (−)-menthylCp.

A contraction of the ring centroid−metal−ring centroid angle is common[13,46] on proceeding from Cp′$_2$LnX complexes (∠Cg1−Ln−Cg2 = 134−140°) to ring-linked *ansa*-metallocenes such as **2b**; however, ∠Cg1−Lu(1)−Cg2 = 122.1(4)° in **2b** is significantly *smaller* than in both $Me_2$SiCp″CpLu($\mu$-Cl)$_2$Li(OEt$_2$)$_2$ (125.2°)[27] and (*R*)-$Me_2$SiCp″[(+)-neomenthylCp]Lu($\mu$-Cl)$_2$Li(OEt$_2$)$_2$ (125.4°).[26a] In fact, it falls closer to the range usually found for ring-linked complexes of the larger lanthanides, e.g., $Me_2$SiCp″(R*Cp)Sm-CH(SiMe$_3$)$_2$ (R* = (+)-neomenthyl, (−)-menthyl) (119.3−121.3°),[26a] suggesting a similar degree of steric unsaturation in **2b**, despite the smaller ionic radius[49] of the lutetium ion in the latter.

The Lu(1)−$C_{ring}$ distances in **2b** (2.55−2.66 Å) are within the range expected for lutetium *ansa*-metallocenes.[26a,27,46] Metal−carbon bond distances between Lu(1) and C(1)−C(5) of the $Me_3$SiCp ring display the typical dispersion pattern observed for similar ring-linked organolanthanide metallocenes;[26,27] the Lu(1)−C(3) (2.66(1) Å) and Lu(1)−C(4) (2.65(1) Å) bonds distal to the $Me_2$Si bridge are slightly longer than the proximal Lu(1)−C(2) (2.56(1) Å) and Lu(1)−C(5) (2.603(9) Å) distances. The (−)-menthylCp ring, however, is canted with longer Lu(1)-C(14) (2.66(1) Å) and Lu(1)-C(15) (2.600(10) Å) distances on the (−)-menthyl-substituted side of the ring and shorter Lu(1)−C(12) (2.56(1) Å) and Lu(1)−C(13) (2.57(1) Å) on the unsubstituted side of the ring. The structures of various $Me_2$SiCp″(R*Cp)-based compounds[26a] exhibit a similar canting of the R*Cp ring. The angles ∠Lu(1)−C(3)−Si(2) (129.4(5)°) and ∠Lu(1)−C(14)−C(16) (127.1(8)°) are significantly larger than the corresponding ∠Lu-$C_{ring}$−$C_{methyl}$ (120.8°) and ∠Ln−$C_{ring}$−$C_{neomenthyl}$ (119.7°) in (*R*)-$Me_2$SiCp″[(+)-neomenthylCp]Lu($\mu$-Cl)$_2$Li(OEt$_2$)$_2$,[26a] further evidencing the repulsive interactions between Cl(1) and the chiral ring auxiliaries.

The cyclohexyl ring of the (−)-menthyl auxiliary, as expected, adopts a chair conformation in which all substituents are in equatorial positions and the isopropyl group is oriented predominantly *anti* to the $Me_2$Si bridge ("$^i$Pr forward", **18** in eq 4).[26a] Close nonbonded contacts between Cl(1) and C(21) (3.70 Å), C(15) and C(21) (2.94 Å), and C(13) and C(23) (3.12 Å) suggest that the observed orientation minimizes unfavorable interactions likely to arise between the bulky isopropyl group

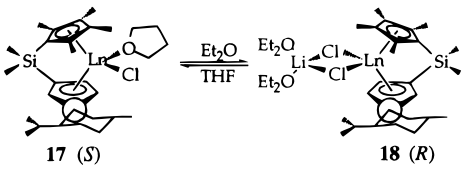


**17** (*S*) **18** (*R*) (4)

and C(15) in a *syn* ("$^i$Pr back", **17** in eq 4)[26a] orientation. Both *anti* and *syn* orientations of the (+)-neomenthyl and (−)-menthyl groups are observed in the diffraction determined structures of (*R*)- and (*S*)-$Me_2$SiCp″(R*Cp)-LnE(SiMe$_3$)$_2$ (Ln = Sm, Y; E = CH, N).[26a]

**Synthesis of Chiral Organolanthanide Hydrocarbyls.** Alkylation of the chloro complexes **2** with 1 equiv of LiCH(SiMe$_3$)$_2$ in toluene followed by extraction with pentane affords the alkyls **3** in essentially quantitative yield (eq 5). The nearly unlimited solubility of

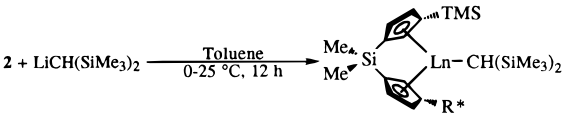


(5)

**3a** Ln = Y
**b** Ln = Lu

**3** in ethereal and hydrocarbon solvents has precluded isolation in crystalline form; analytical and spectroscopic data, however, affirm their chemical purity (see Experimental Section for details).

Like the chloro precursor complexes **2**, epimerically pure **3** should in principle display 6 multiplets in the cyclopentadienyl region of the $^1$H NMR spectrum. The observation of twice the expected number of cyclopentadienyl resonances in the room-temperature $^1$H NMR spectrum of **3b** (see Experimental Section for data) would seem at first to indicate that epimerization occurs during alkylation. Alkylation of related (*R*)- or 70/30 (*S*)/(*R*)-$Me_2$SiCp″[(−)-menthylCp]Ln($\mu$-Cl)$_2$Li(OEt$_2$)$_2$ complexes, however, is known to proceed with retention of configuration (i.e., without epimerization of the (−)-menthylCp attachment mode) under identical reaction conditions.[26a] Furthermore, CD spectroscopy of **3** (Figure 4) argues that the *R* configuration of the R*CpLn fragment still predominates. In the present case, the possibility of epimerization of the $Me_3$SiCp attachment mode cannot be dismissed *a priori*; however, variable-temperature $^1$H NMR studies (Figure 5) reveal that, rather than epimerization of either Cp ring, the additional signals arise from structures which undergo temperature-dependent interchange. At −20 °C, the 12 cyclopentadienyl resonances in the $\delta$ 5.9−6.9 ppm region (Figure 5A) are sharp and well resolved, while the presence of 10 sharp singlets in the $\delta$ 0.0−0.7 ppm range (Figure 5B) is consistent with *two* sets each of the resonances attributable to the diastereotopic silyl methyls of both bridge and hydrocarbyl SiMe$_3$ groups as well as two resonances for the $Me_3$SiCp methyls. As the temperature is raised to 40 °C, the cyclopentadienyl signals, as well as those in the upfield portion of the spectrum, broaden and begin to collapse. At 100 °C, the cyclopentadienyl resonances have nearly coalesced into 6 signals, and only two signals remain corresponding to the diastereotopic bridge methyls; the $Me_3$Si signals from both the hydrocarbyl and Cp ring auxiliary are contained in one large, broad singlet ($\delta$ 0.14 ppm), and the three methyl doublets of the (−)-menthyl auxiliary,

(49) Shannon, R. E. *Acta Crystallogr.* **1976**, *A32*, 751−760.

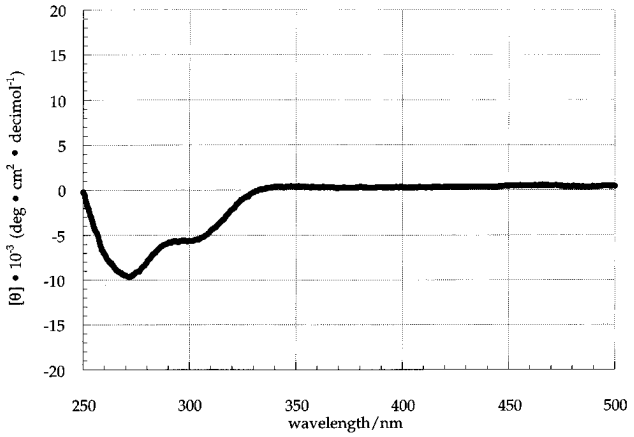


**Figure 4.** Circular dichroism spectrum of $Me_2Si(Me_3SiCp)$[(−)-menthylCp]LuCH$(SiMe_3)_2$ (**3b**) in heptane at 25 °C.

obscured in the lower temperature spectra, are now clearly visible. The reverse of this process is observed as the temperature is subsequently reduced from 100 to −20 °C.

The observed exchange process in **3** is likely the result of conformational isomerism arising from rotation about the Ln−CH$(SiMe_3)_2$ $\sigma$-bond, similar to that seen in CH$(SiMe_3)_2$-substituted zirconocenes.[50] Homonuclear decoupling experiments performed at low temperature in the $^1$H NMR spectra of **3** confirm the presence of four sets of three coupled signals. For the Y complex **3a**, two sets account for ∼55% of the signal intensity and the other two sets account for the remaining ∼45%. In the Lu analog **3b**, the corresponding resonances are present in proportions of ∼60% and ∼40%. Also present in both spectra are small (<5% of major conformer signal intensity) resonances which could be attributable to a third conformer and which do not appear to undergo rapid exchange with the other two structures. Similar features are detected in the $^1$H NMR spectra of (*R*/*S*)-$Me_2SiCp''$[(+)-neomenthylCp]LnCH$(SiMe_3)_2$ complexes (Ln = Y, Lu)[26] and are attributed to a minor configurational isomer.[51]

Consistent with the above observations, an examination of the three most reasonable structures (**19**−**21**)

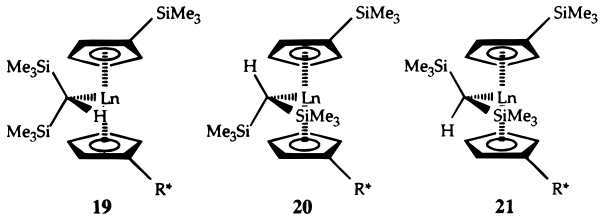


reveals that, on steric grounds, **19** should be the least probable of the three, since the $SiMe_3$ groups would both encounter significant nonbonded repulsions from the cyclopentadienyl hydrogen atoms toward the rear of the metallocene "clamshell". Isomers **20** and **21** can mitigate these unfavorable interactions by placing one $SiMe_3$ group into the relatively open volume at the front of the clamshell, while the other occupies a site distal to either the ring $SiMe_3$ or (−)-menthyl auxiliary, reminiscent of the structures of $Me_2SiCp''$(R*Cp)LnCH$(SiMe_3)_2$ complexes.[26a] Indeed, the crystal structures of a variety of lanthanocene hydrocarbyls all reflect a minimization of hydrocarbyl group−ring substituent interactions; in the structure of $Me_2SiCp''$CpLuCH$(SiMe_3)_2$,[27] for example, the $SiMe_3$ groups of the hydrocarbyl are oriented away from the Cp″ methyl substituents. This preference appears to persist in the solution phase where NMR reveals that population of the other CH$(SiMe_3)_2$ conformation is minor at most.[26a,27]

At 25 °C, complex **3a** is in the intermediate exchange regime, while complex **3b** is at slow exchange. This is not surprising as the larger eight-coordinate ionic radius[49] of $Y^{3+}$ (1.019 Å) versus that of $Lu^{3+}$ (0.977 Å) and the correspondingly longer metal−ligand distances

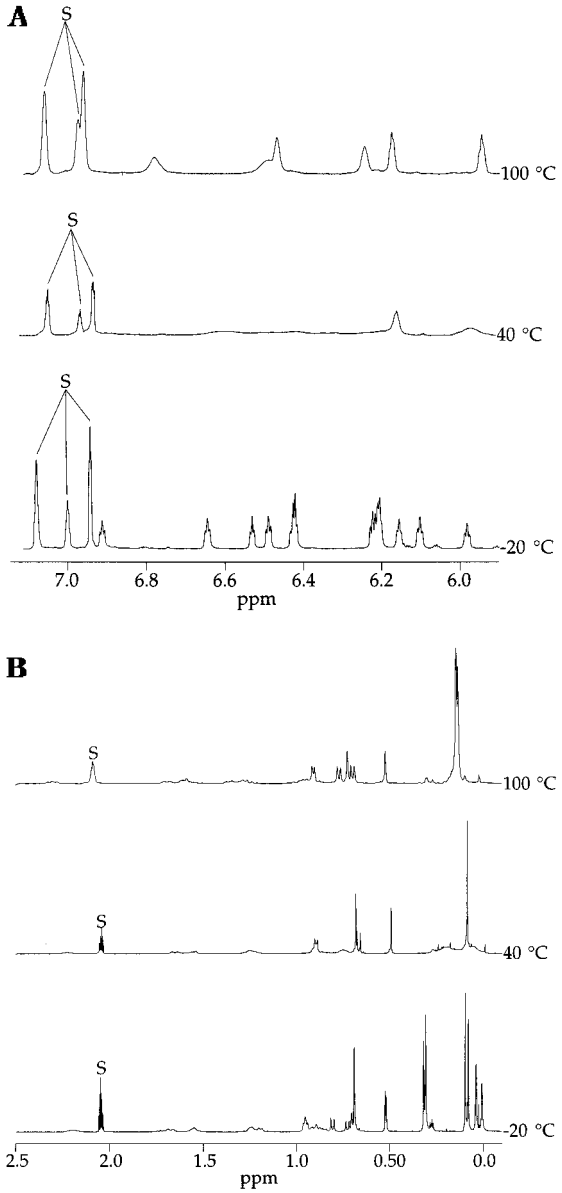


**Figure 5.** Variable-temperature $^1$H NMR spectra (400 MHz) of (*S*,*R*)-$Me_2Si(Me_3SiCp)$[(−)-menthylCp]YCH$(SiMe_3)_2$ (**3a**) in toluene-$d_8$ at −20, 40, and 100 °C: (A) Cyclopentadienyl region; (B) aliphatic region. S indicates solvent resonances.

(50) (a) Lappert, M. F.; Riley, P. I.; Yarrow, P. I. W.; Atwood, J. L.; Hunter, W. E.; Zaworotko, M. J. *J. Chem. Soc., Dalton Trans.* **1981**, 814−821. (b) Jeffery, J.; Lappert, M. J.; Luong-Thi, N. T.; Atwood, J. L.; Hunter, W. E. *J. Chem. Soc., Chem. Commun.* **1978**, 1081−1083.

(51) Note that in the $^1$H NMR spectrum of $Me_2Si(Me_3SiCp)$[(−)-menthylCp]YCH$_2$P$Me_2$, which contains a Lewis basic phosphorus capable of interacting with the Lewis acidic $Y^{3+}$ ion, only 6 cyclopentadienyl resonances are observed over the range 25−90 °C: Haar, C. M.; Marks, T. J. Unpublished observations.

Downloaded by CARLI CONSORTIUM on June 30, 2009
Published on April 2, 1996 on http://pubs.acs.org | doi: 10.1021/om950871v

would be expected to more readily accommodate rotation of the $CH(SiMe_3)_2$ group. The converse of this effect is also seen in the slightly stronger bias toward a (limiting) single conformer in **3b** and in the higher catalytic enantioselection exhibited by the Lu catalyst (*vide infra*). In the more sterically demanding environments of $Cp'_2$-, $Me_2SiCp''_2$-, and $Me_2SiCp''$(R*Cp)-ligated lanthanide hydrocarbyls, such a rotation process is doubtless arrested by the greater steric congestion.

**Reaction of Hydrocarbyl Complexes with Hydrogen.** Solutions of **3** in hydrocarbon solvents undergo slow hydrogenolytic cleavage of the hydrocarbyl group to quantitatively afford putative hydrido complex **4** (eq 6) as evidenced by the appearance of $CH_2(SiMe_3)_2$ in the

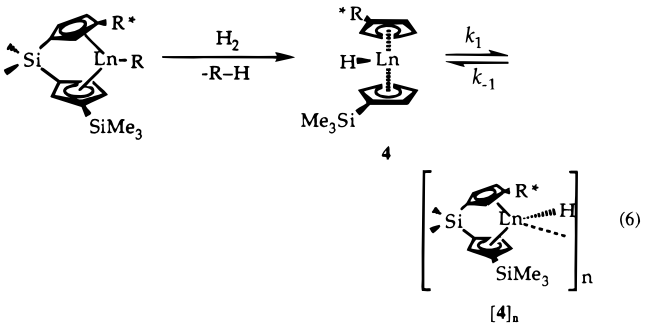


(6)

solution $^1$H NMR (taken in $C_6D_{12}$ or $C_6D_{11}CD_3$ to avoid H/D exchange between the hydrido complex and deuterated aromatic solvents). The $^1$H NMR spectrum of **4** at 25 °C contains one very broad peak ($\delta$ 5.6−7.4 ppm) in the cyclopentadienyl region, while the upfield portion displays a large number of sharp, though poorly resolved, resonances. This is in contrast to well-characterized $(Cp'_2LnH)_2$,[13] $(Me_2SiCp''_2LnH)_2$,[15] $(Me_2SiCp''CpLnH)_2$,[27] and $[Me_2SiCp''(R*Cp)LnH]_2$,[26a] the NMR spectra of which are readily interpretable as arising from tightly ($k_1 > k_{-1}$) associated hydrido-bridging dimers. The characteristic triplet found in the spectra of $(Et_2SiCp''CpYH)_2$[27] ($\delta$ 3.03 ppm; $^1J_{^{89}Y-^1H} = 35$ Hz), $[Me_2SiCp''(R*Cp)YH]_2$[26a] ($\delta$ 4.28 ppm; $^1J_{^{89}Y-^1H} = 32$ Hz), and $[Cp'(2,6\text{-}{}^tBu_2C_6H_3O)YH]_2$[29] ($\delta$ 5.64 ppm; $^1J_{^{89}Y-^1H} = 35.2$ Hz), indicative of a Y($\mu$-H)Y bonding motif in these compounds, is absent in the present case to temperatures as low as −75 °C. At this temperature, several broad resonances are visible in the cyclopentadienyl region; however, they offer no clear evidence of well-defined bimolecular species. While these data could be consistent with higher order oligomers or high molecular weight polymers, the coordinative unsaturation also raises the possibility of catalyst self-destruction *via* internal metalation,[52] or a combination of both factors.

**Catalytic Hydrogenation. Reductive Cyclization of α,ω-Diolefins.** The comparatively sluggish hydrogenolysis of $Ln-CH(SiMe_3)_2$ observed in the present NMR studies of **3** + $H_2$ as well as the kinetics of **3**-catalyzed hydrogenation of 2-phenyl-1-butene (*vide infra*) suggests that **3** might be an ideal precatalyst for the reductive cyclization of α,ω-diolefins (eq 7), as the cyclization step (intramolecular insertion of the terminal C=C into the Ln−C bond) in the catalytic cycle might become competitive with Ln−C hydrogenolysis. In the

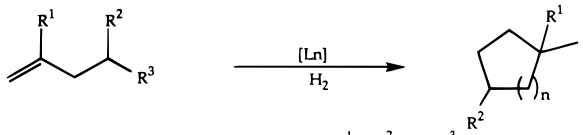


(7)

$R^1 = R^2 = H$, $R^3 = CHCH_2$; n = 1
$R^1 = Me$, $R^2 = H$, $R^3 = CHCH_2$; n = 1
$R^1 = H$, $R^2 = OSiMe_2{}^tBu$, $R^3 = CH_2CHCH_2$; n = 2

case of reductive cyclizations mediated by $Cp'_2YH(THF)$,[24] the presence of the coordinated Lewis base THF apparently serves to depress the rate of Ln−C hydrogenolysis more than that of olefin insertion;[16a] in the present case, the increased hardness/decreased electron donor power of the ancillary ligation might also moderate reactivity.[29,43]

Exposure to $H_2$ (1 atm) of neat 1,5-hexadiene or 2-methyl-1,5-hexadiene solutions of precatalyst **3** (~200:1 substrate:catalyst ratio) results in the quantitative conversion of the respective diolefins to methylcyclopentane or 1,1-dimethylcyclopentane within 2 h at 22 °C (Table 3). Attempts to cyclize *tert*-butyldimethylsilyl-(TBDMS) protected hepta-1,6-dien-4-ol resulted in the quantitative recovery of unaltered substrate. Despite the demanding steric encumbrance of the TBDMS ether moiety, the relatively open coordination environment and extreme Lewis acidity of the metal center apparently invites coordinative inhibition by any available base. In fact, the presence of any Lewis base in the coordination sphere of **3** or **4** completely suppresses olefin hydrogenation activity—a catalytic trial inadvertently performed with 2-phenyl-1-butene contaminated with <1% (by NMR) diethyl ether also exhibited negligible turnover. This behavior stands in contrast to $Cp'_2Ln$- and $Me_2SiCp''_2Ln$-based catalysts where activity for 1-hexene hydrogenation is reduced only by a factor of ~16 when reactions are performed with THF as the solvent.[16a]

**Enantioselective Reduction of Prochiral Olefins.** The efficacy of the present chiral complexes $Me_2Si(Me_3Si)Cp[(-)\text{-menthylCp}]LnCH(SiMe_3)_2$ (**3**) as precatalysts for asymmetric olefin hydrogenation and deuteration was assayed with the unfunctionalized olefins 2-phenyl-1-butene, styrene, 2-ethyl-1-hexene, and 1-pentene (eqs 8−11). These unfunctionalized

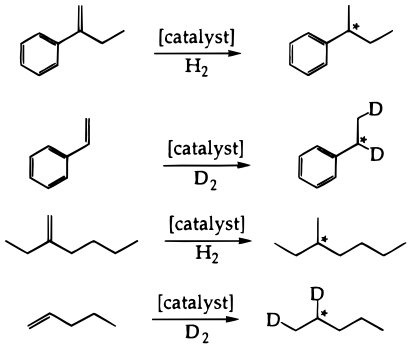


(8)

(9)

(10)

(11)

olefins are typically difficult substrates to reduce with substantial enantioselectivity and at appreciable rates.[3,53] In a typical procedure, a 200:1 molar ratio of substrate:catalyst was employed in neat olefin or pentane solution with $P_{H_2} = 1$ atm and rapid stirring. The substrates

(52) (a) Schock, L. E.; Brock, C. P.; Marks, T. J. *Organometallics* **1987**, *6*, 232. (b) McDade, C.; Brock, C. P.; Bercaw, J. E. *Organometallics* **1982**, *1*, 1629.

(53) (a) Bakos, J.; Tóth, I.; Heil, B.; Markó, L. *J. Organomet. Chem.* **1985**, *279*, 23−29. (b) Hayashi, T.; Tanaka, M.; Ogata, I. *Tetrahedron Lett.* **1977**, *18*, 295−296.

Downloaded by CARLI CONSORTIUM on June 30, 2009
Published on April 2, 1996 on http://pubs.acs.org | doi: 10.1021/om950871v

**Table 3. Data for the Reductive Cyclization of Various 1,5- and 1,6-Diolefins Mediated by (*S*,*R*)-Me$_2$Si(Me$_3$SiCp)[(−)-menthylCp]LnCH(SiMe$_3$)$_2$ (3) Precatalysts[a]**

| entry | substrate | product | precatalyst | yield (%)[b] |
|---|---|---|---|---|
| 1 | 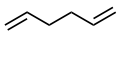 |  | **3a** | 100 |
| | | | **3b** | 100 |
| 2 | 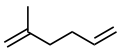 |  | **3a** | 100 |
| | | | **3b** | 100 |
| 3 | 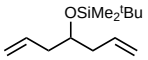 | 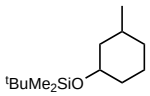 | **3a** | 0[c] |
| | | | **3b** | 0[c] |

[a] Conditions: [substrate]/[catalyst] = 200/1; $P_{H_2}$ = 750 Torr; rapid stirring. [b] Conversions determined by GLC and $^1$H NMR. [c] Solvent = *n*-pentane.

2-phenyl-1-butene, styrene, and 2-ethyl-1-hexene undergo clean, quantitative conversion to 2-phenylbutane, ethylbenzene, and 3-methylheptane, respectively. The catalytic reduction of neat 1-pentene, however, does not proceed in quantitative yield. In each catalytic trial yields of pentane-1,2-$d_2$ varied between ∼70 and 90%. A clear, involatile liquid—sometimes tinted yellow with organolanthanide residues—remained in the reaction tube after the removal *in vacuo* of all volatile components and accounted for the remaining reaction mass. $^1$H NMR of this substance shows no evidence of olefinic signals, only many large, overlapping aliphatic signals in the upfield portion of the spectrum. Similarly, the GC of such a sample displays several peaks at very long retention times compared to *n*-pentane solvent.

These observations are consistent with a competing insertive olefin oligomerization pathway similar to that observed for (Cp′$_2$LnH)$_2$ and (Me$_2$SiCp″$_2$LnH)$_2$ under conditions of hydrogen starvation (eq 12).[13a,b,14,15,17] The

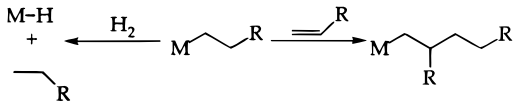

(12)

slow rate of Ln−C hydrogenolysis in the present case is operationally equivalent to hydrogen starvation of the catalyst. Taking into account the decreased steric requirements of the Me$_2$Si(Me$_3$SiCp)[(−)-menthylCp] ligand and the high substrate concentrations, the insertion of another pentene into an existing Ln−C$_5$H$_{11}$ could become competitive with product-liberating hydrogenolysis, leading to the formation of light oligomers. Furthermore, the regiospecific formation of reduction products ethylbenzene-1,2-$d_2$ and pentane-1,2-$d_2$ (by $^{13}$C NMR) in addition to the lack of olefinic resonances in the NMR spectrum of the oligomeric 1-pentene products, argues that $\beta$-hydride elimination/readdition does not effectively compete with hydrogenolysis of the intermediate Ln alkyl formed by olefin insertion. This is further supported by the observation that negligible quantities of 2-phenylbutane-$d_{>2}$ are found in GC/MS analysis of the reaction mixture from deuteration of 2-phenyl-1-butene with **3a**.

Presumably, the catalytically active species in the present case is a Ln hydride generated *via* hydrogenolysis (eq 6) of the hydrocarbyl precatalysts (*vide supra*).[13,26a] $^1$H NMR spectra of the organometallic residues remaining after vacuum transfer of volatiles from the reaction mixtures are similar to those of the hydrides (**4**), but equally uninformative. Like (Cp′$_2$LnH)$_2$ or (Me$_2$SiCp″$_2$LnH)$_2$ systems, residual solutions of **4a** exhibit activities identical to those of the *in situ* generated catalyst[16] but, interestingly, only after an induction period of several minutes following substrate addition (*vide infra*). In contrast, the hydrides [Me$_2$SiCp″(R*Cp)LnH]$_2$,[26] [Me$_2$Si(1-(Me$_3$Si)-3-$^t$BuCp)$_2$YH]$_2$,[25] and (Me$_2$SiCp″CpLnH)$_2$[27] display a marked, essentially irreversible decline in catalytic activity of preformed hydrides which is attributed to the formation of various tightly associated ($\mu$-H)$_2$ species.

**Table 4. Product Enantiomeric Excess (ee) and Absolute Configuration Data for Hydrogenation of 2-Phenyl-1-butene and 2-Ethyl-1-hexene and Deuteration of Styrene and 1-Pentene with (*S*,*R*)-Me$_2$Si(Me$_3$SiCp)[(−)-menthylCp]LnCH(SiMe$_3$)$_2$ (3) Precatalysts[a]**

| entry | substrate | Ln | *T* (°C) | ee (%) (sign) |
|---|---|---|---|---|
| 1 | α-ethylstyrene | Y | 22 | 25 (*S*)[d] |
| 2 | α-ethylstyrene | Y | 25 | 28 (*S*)[e,f] |
| 3 | α-ethylstyrene | Y | 22 | 28 (*S*)[b,g] |
| 4 | α-ethylstyrene | Lu | 22 | 45 (*S*)[d] |
| 5 | styrene | Y | 22 | 3 (*S*)[d] |
| 6 | styrene | Lu | 22 | 10 (*R*)[d] |
| 7 | 1-pentene | Y | 0 | 16 (*S*)[b,c] |
| 8 | 1-pentene | Lu | 0 | 30 (*S*)[b,c] |
| 9 | 2-ethyl-1-hexene | Y | 22 | <1 (−)[b] |
| 10 | 2-ethyl-1-hexene | Lu | 22 | 2.4 (−)[b] |

[a] Conditions: [substrate]/[catalyst] = (100−1000)/1; $P_{H_2}$ = 750 Torr; rapid stirring; 100% conversion by GLC and $^1$H NMR. [b] Solvent = substrate. [c] Oligomeric products also found. [d] Solvent = *n*-pentane. [e] Solvent = *n*-heptane. [f] Vortex mixing.[16a] [g] $P_{H_2}$ = 180 psi.

Table 4 lists the results of asymmetric hydrogenation and deuteration experiments with a variety of styrenic and non-styrenic substrates mediated by precatalysts **3**. Most notable are the significant enantioselectivities afforded by the present *meso* configuration of the ligand−metal template. Despite the traditional difficulty encountered in reducing such nonpolar olefins with appreciable asymmetric induction,[3,53] enantioselectivities for the hydrogenation of 2-phenyl-1-butene by (*S*,*R*)-{Me$_2$Si(Me$_3$SiCp)[(−)-menthylCp]LnH}$_2$ (28% ee (*S*), **3a**; 45% ee (*S*), **3b**) are significant and exceed selectivities of the analogous Me$_2$SiCp″(R*Cp)Ln−catalyzed reactions where Ln = Y and Lu and R* = (+)-neomenthyl and (−)-menthyl.[26b] The deuteration of styrene mediated by **3**, however, proceeds with lower enantioselectivity (3% ee (*S*), **3a**; 10% ee (*R*), **3b**) and, in the case of precatalyst **3b**, yields a product enriched in the *opposite* configuration from that expected on the basis of the results for 2-phenyl-1-butene. In contrast, the (*R*)- or 70/30 (*S*/*R*)-Me$_2$SiCp″[(−)-menthylCp]Sm-catalyzed reduction of styrene (43% ee (*R*), 72% ee (*S*), respectively)[26b] proceeds with *higher* enantioselectivity than that of 2-phenyl-1-butene, while the absolute configurations of the respective predominant products can be rationalized in terms of similar interactions between substrate molecules and the chiral catalyst configuration (*vide infra*). Note, however, that the enantioselectivity of precatalyst **3** *increases* with decreasing lanthanide ionic radius for all substrates, in contrast to Me$_2$SiCp″[(+)-neomenthylCp]Ln-based catalysts where an approximately direct relationship between Ln$^{3+}$ ionic radius and enantioselectivity is observed.[26] Also, no effect of mixing speed or $H_2$ pressure on % ee was found for the hydrogenation of 2-phenyl-

Downloaded by CARLI CONSORTIUM on June 30, 2009
Published on April 2, 1996 on http://pubs.acs.org | doi: 10.1021/om950871v

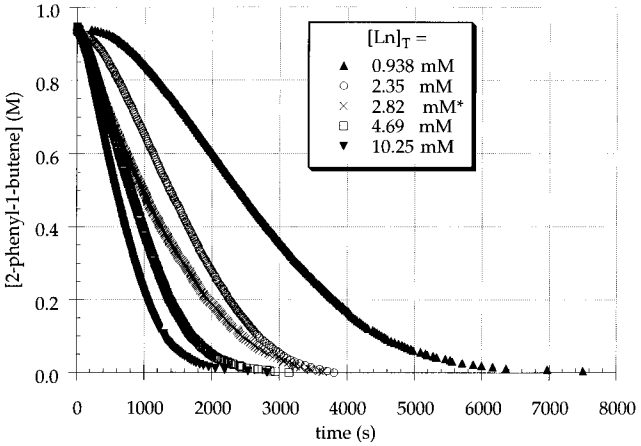


**Figure 6.** Plot of 2-phenyl-1-butene concentration as a function of time at various indicated total precatalyst concentrations and 700 Torr total hydrogen pressure for the catalytic asymmetric hydrogenation of 2-phenyl-1-butene mediated by (*S*,*R*)-$Me_2Si(Me_3SiCp)$[(−)-menthylCp]-$YCH(SiMe_3)_2$. * indicates vortex mixing was used.

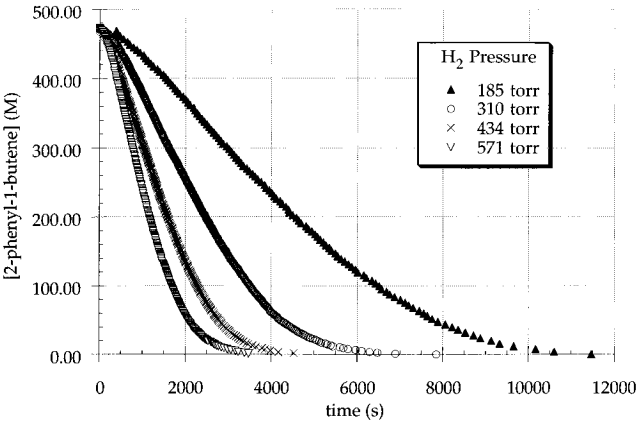


**Figure 7.** Plot of 2-phenyl-1-butene concentration as a function of time at various indicated total hydrogen pressures and 2.56 mM total precatalyst concentration for the catalytic asymmetric hydrogenation of 2-phenyl-1-butene mediated by (*S*,*R*)-$Me_2Si(Me_3SiCp)$[(−)-menthylCp]YCH-$(SiMe_3)_2$.

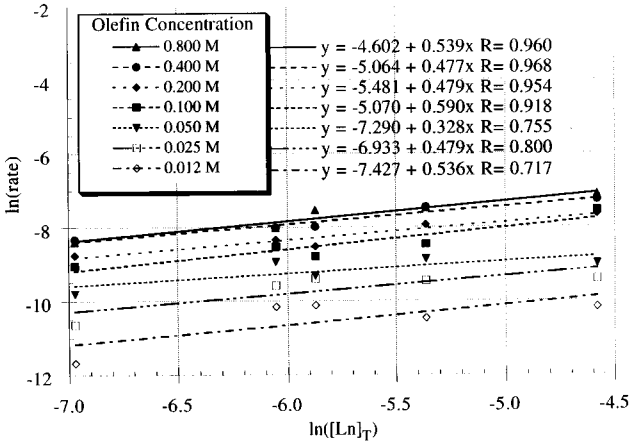


**Figure 8.** Van't Hoff plots at various indicated olefin concentrations for the lanthanide concentration dependence of the catalytic asymmetric hydrogenation of 2-phenyl-1-butene mediated by (*S*,*R*)-$Me_2Si(Me_3SiCp)$[(−)-menthylCp]-$YCH(SiMe_3)_2$.

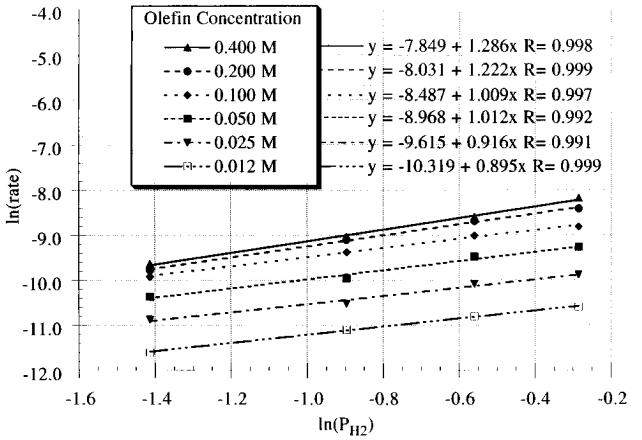


**Figure 9.** Van't Hoff plots at various indicated olefin concentrations for the hydrogen pressure dependence of the catalytic asymmetric hydrogenation of 2-phenyl-1-butene mediated by (*S*,*R*)-$Me_2Si(Me_3SiCp)$[(−)-menthylCp]YCH-$(SiMe_3)_2$.

1-butene with **3a** as precatalyst when the reaction was performed at $P_{H_2} = 1$ atm with slow stirring (25% ee (*S*)) and in a well-mixed (vortex) batch reactor[16a] (28% ee (*S*)) or when stirred under $P_{H_2} = 10$ atm (27% ee (*S*)).

The deuteration of 1-pentene by **3a** (16% ee (*S*)) and **3b** (30% ee (*S*)) obeys stereoselection rules similar to those of the styrenic substrates, including higher selectivity of the smaller Lu catalyst. Hydrogenation of 2-ethyl-1-hexene, however, proceeds with only minimal enantioselection (<1% ee (−), **3a**; 2.4% ee (−), **3b**). Although the absolute configuration of (+)- or (−)-3-methylheptane has not yet been confirmed, the rotations observed in both **3a**- and **3b**-derived 3-methylheptane are in the same direction, indicating that the putatively isostructural Y and Lu catalysts mediate preferential atom transfer to the same enantioface of the olefin. The modest increased enantioselectivity of **3b** over **3a** in the hydrogenation of 2-ethyl-1-hexene also conforms to the ionic radius trend established for the reduction of the styrenic substrates above.

**Kinetics of Organolanthanide-Catalyzed Enantioselective Hydrogenation.** The kinetics of the asymmetric hydrogenation of 2-phenyl-1-butene with $Me_2Si(Me_3SiCp)$[(−)-menthylCp]$YCH(SiMe_3)_2$ (**3a**) were studied to obtain turnover frequency data and to establish the empirical rate law. A constant pressure (pseudo-zero order in $H_2$ pressure), stirred or vortex-mixed batch reactor was employed using procedures described previously (see Experimental Section for details).[16b] Typical kinetic plots for the consumption of olefin during hydrogenation at various initial precatalyst concentrations (Figure 6) and hydrogen pressures (Figure 7) are sigmoidal, with an induction period of ~5−10 min. When $D_2$ is used, the induction period is significantly longer, ~30 min. Following initiation, the rate of substrate consumption ($v$) is constant (zero-order behavior) through approximately one half-life and then begins gradually to deviate from linearity. This behavior is clearly more complex than reduction of the same substrate with $Me_2SiCp''(R^*Cp)Ln$-based catalysts, where the behavior is zero-order in olefin (linear consumption plot) over the entire conversion range.[26b] Note in the present case that hydrogenation performed under non-mass transport limited (very fast vortex mixing) conditions is not significantly faster than the stirred reactions under otherwise similar conditions. The turnover frequency ($N_t$, $h^{-1}$) depends on the total lanthanide con-

Downloaded by CARLI CONSORTIUM on June 30, 2009
Published on April 2, 1996 on http://pubs.acs.org | doi: 10.1021/om950871v

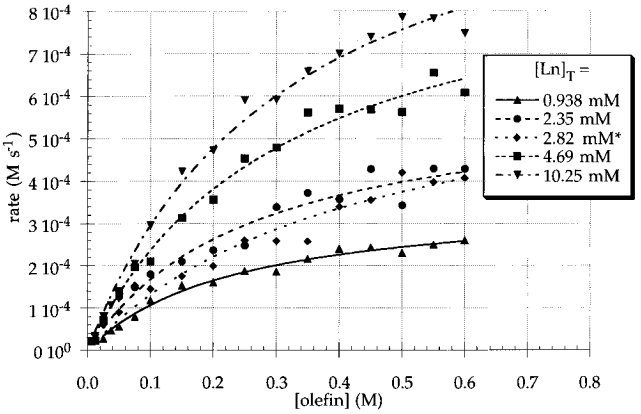


**Figure 10.** Rate as a function of 2-phenyl-1-butene concentration at various total precatalyst concentrations and 700 Torr total hydrogen pressure for the catalytic asymmetric hydrogenation of 2-phenyl-1-butene mediated by (*S*,*R*)-$Me_2Si(Me_3SiCp)$[(−)-menthylCp]YCH$(SiMe_3)_2$. Curves are drawn as a guide to the eye. * indicates vortex mixing was used.

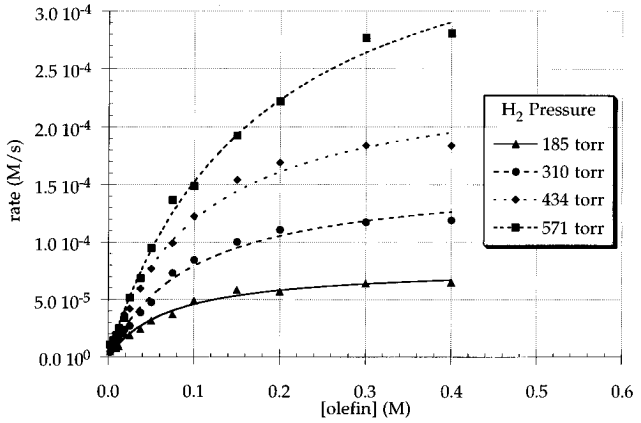


**Figure 11.** Rate as a function of 2-phenyl-1-butene concentration at various total hydrogen pressures and 2.56 mM total precatalyst concentration for the catalytic asymmetric hydrogenation of 2-phenyl-1-butene mediated by (*S*,*R*)-$Me_2Si(Me_3SiCp)$[(−)-menthylCp]YCH$(SiMe_3)_2$. Curves are drawn as a guide to the eye.

centration, with a maximum turnover frequency ($N_t$ = 860 $h^{-1}$) observed for $[Ln]_T$ = 0.938 mM. Van't Hoff treatment of the rate data, obtained at constant $H_2$ pressure and in which the initial concentration of **3a** was varied from 0.938 to 10.25 mM, supports a reaction order of ∼0.5 in total lanthanide concentration over olefin concentrations ranging from ∼0.01 to ∼0.8 M (Figure 8). Similar treatment of data obtained at constant total lanthanide concentration over a 0.243−0.921 atm $H_2$ pressure range support an approximately first-order dependence in $H_2$ at olefin concentrations from ∼0.01 to ∼0.4 M (Figure 9). Although the derived order in $H_2$ may trend slightly downward at lowest olefin concentrations, the differences are on the edge of statistical significance (the median of the standard deviations of the slopes determined in Figure 9 is on the order of 0.2 at 95% confidence). Additionally, a significant $H_2/D_2$ kinetic isotope effect (KIE) for the catalytic hydrogenation process ($v_{H_2}/v_{D_2}$ = 2.17; [olefin] = 0.800 M at 25.0 ± 0.2°C) is observed. For the

(54) Segel, I. H. *Enzyme Kinetics*; Wiley: New York, 1975; Chapters 2, 9.

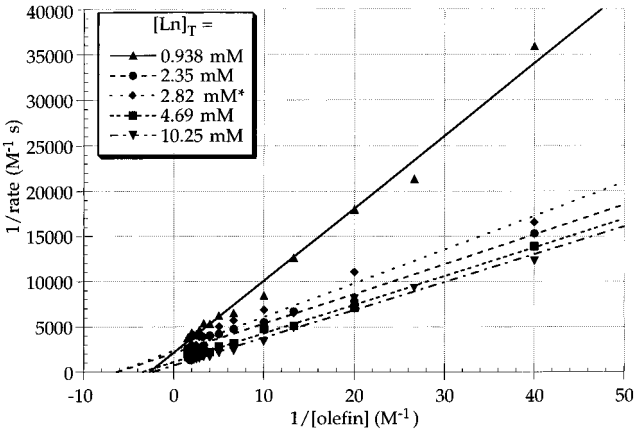


**Figure 12.** Lineweaver−Burk double reciprocal plots of rate *vs.* 2-phenyl-1-butene concentration at various indicated lanthanide concentrations and 700 Torr total hydrogen pressure for the catalytic asymmetric hydrogenation of 2-phenyl-1-butene mediated by (*S*,*R*)-$Me_2Si(Me_3SiCp)$-[(−)-menthylCp]YCH$(SiMe_3)_2$. * indicates vortex mixing was used.

moment, including the olefin-dependent term in $k_{obs}$, the above data support the rate law of eq 13.

$$v = k_{obs}[Ln]_T^{1/2}[H_2]^1 \qquad (13)$$

The sigmoidicity of the substrate consumption curves (Figures 6 and 7) clearly indicates the olefin dependence of the reaction rate is complex. Although neither zero-order nor first-order plots appear to model this behavior convincingly over the entire conversion range, they do suggest a gradual shift from an olefin-independent regime at higher concentrations to an approximately first-order dependence as substrate is depleted. Plots of the present rate data as a function of substrate concentration (Figures 10and 11) illustrate this behavior and are reminiscent of substrate saturation effects frequently observed in enzyme kinetics.[54] In a Henri−Michaelis−Menten description (eqs 14 and 15); E = enzyme, S = substrate, P = product), the Michaelis constant $K_S$ refers to the overall effectiveness of substrate capture summed over all catalyst species, while $V_{max} = k_{app}[E]_T$ refers to the apparent efficiency of the product-forming step. In a simple situation such as eq 14, there is no inhibition of product formation, and $k_{app} = k_p$. At sufficiently high substrate concentrations ([S] ≫ $K_S$), the [S] terms dominate and the rate law becomes zero-order in [S]. At lower [S], approximately first-order behavior is observed.

$$E + S \underset{}{\overset{K_S}{\rightleftharpoons}} ES \xrightarrow{k_p} E + P \qquad (14)$$

$$\frac{v}{V_{max}} = \frac{[S]}{K_s + [S]} \qquad (15a)$$

$$\frac{1}{v} = \frac{K_S}{V_{max}[olefin]} + \frac{1}{V_{max}} \qquad (15b)$$

Recasting the present kinetic data as Lineweaver−Burk double reciprocal plots[54] (Figures 12and 13) yields families of straight lines at constant $[Ln]_T$ and $[H_2]$, in approximate accord with this simple model. $V_{max}$ can be obtained from the 1/*v* intercept and $K_S$ from the 1/[olefin] intercept (eq 15b). Examination of the result-

Downloaded by CARLI CONSORTIUM on June 30, 2009
Published on April 2, 1996 on http://pubs.acs.org | doi: 10.1021/om950871v

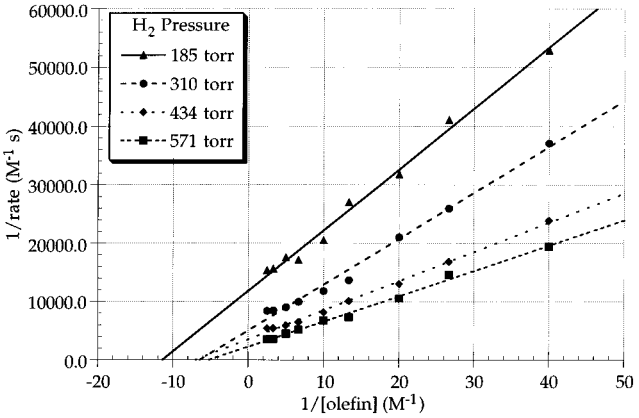


**Figure 13.** Lineweaver−Burk double reciprocal plot of rate *vs.* [2-phenyl-1-butene] data at various indicated total hydrogen pressures and 2.56 mM total lanthanide concentration for the catalytic asymmetric hydrogenation of 2-phenyl-1-butene mediated by (*S*,*R*)-$Me_2Si(Me_3SiCp)$-[(−)-menthylCp]YCH$(SiMe_3)_2$.

**Table 5. Apparent Rate ($V_{max}$, $k_{app}$) and Substrate Dissociation ($K_S$) Constants for the Asymmetric Catalytic Hydrogenation of 2-Phenyl-1-butene Mediated by (*S*,*R*)-$Me_2Si(Me_3SiCp)$[(−)-menthylCp]YCH$(SiMe_3)_2$ (3a) As Determined from Lineweaver−Burk Reciprocal Plots at Various $[Ln]_T$ and $P_{H_2}$ Values**

| entry | $[Ln]_T$ ($\times 10^{-3}$ M) | $P_{H_2}$ (atm) | $V_{max}$ ($\times 10^{-3}$ M s$^{-1}$) | $k_{app}$ ($\times 10^{-3}$ M$^{1/2}$ atm$^{-1}$ s$^{-1}$)[a] | $K_S$ (M) |
|---|---|---|---|---|---|
| 1 | 0.938 | 0.921 | 0.5(1) | 17(5) | 0.4(1) |
| 2 | 2.35 | 0.921 | 0.48(6) | 11(1) | 0.16(2) |
| 3 | 2.82 | 0.921 | 0.42(8) | 9(2) | 0.16(3) |
| 4 | 4.69 | 0.921 | 0.9(1) | 15(2) | 0.29(4) |
| 5 | 10.2 | 0.921 | 1.4(6) | 15(6) | 0.4(2) |
| 6 | 2.56 | 0.243 | 0.08(1) | 6.8(8) | 0.09(1) |
| 7 | 2.56 | 0.408 | 0.20(4) | 10(2) | 0.16(4) |
| 8 | 2.56 | 0.571 | 0.29(4) | 10(1) | 0.14(2) |
| 9 | 2.56 | 0.751 | 0.45(9) | 12(2) | 0.19(4) |
| | | | mean | 12(1) | 0.22(3) |

[a] Calculated from $V_{max} = k_{app}[Ln]_T^{1/2}P_{H_2}$.

ing kinetic parameters (Table 5) reveals that $V_{max}$ increases with $[Ln]_T$ in half-order fashion and approximately monotonically with $P_{H_2}$, in accord with eq 13. Averaging the results of all entries in Table 5 yields $k_{app} = 12(1) \times 10^{-3}$ M$^{1/2}$ atm$^{-1}$ s$^{-1}$ and $K_S = 0.22(3)$ M, where $k_{app}$ in this case is the apparent rate constant derived from $V_{max} = k_{app}[Ln]_T^{1/2}[H_2]$. This expression is essentially identical to eq 13 in that $k_{obs} = k_{app}$ at saturating substrate concentrations. Combining the "classical" organolanthanide rate law of eq 13 with eq 15a yields the empirical rate law (eq 16) for the hydrogenation of 2-phenyl-1-butene by **3a**.

$$v = \frac{k_{app}[\text{olefin}][Ln]_T^{1/2}[H_2]}{K_s + [\text{olefin}]} \qquad (16)$$

Although the hydrides **4** could not be isolated, their catalytic activity for the hydrogenation of 2-phenyl-1-butene was indistinguishable regardless of whether the catalyst was preformed or formed *in situ* by hydrogenolysis of the alkyl precursor. In one experiment, the rate of hydrogen uptake was monitored (see Experimental Section) for the hydrogenation of an aliquot of 2-phenyl-1-butene solution. After $H_2$ uptake had ceased, a second (∼10% of the total reaction volume) aliquot of substrate was added; $H_2$ uptake resumed at a slow rate but then accelerated until the second $H_2$ uptake curve was indistinguishable from the first.

## Discussion

**Catalyst Configurational Stability and Epimerization.** It was shown in NMR spectroscopic and crystallographic studies of chiral $Me_2SiCp''$[(−)-menthylCp]Ln$(\mu\text{-Cl})_2$Li(solvent)$_2$ complexes[26a] that the solvent identity, not $Ln^{3+}$, primarily determines the preference for lanthanide ion coordination to one diastereoface or the other of the (−)menthylCp ring in solution. At equilibrium in THF solution, the (*S*) attachment mode is favored by ∼ 6:1 over the (*R*), while in diethyl ether, the situation is reversed with the (*R*) configuration being the exclusive (>95%) product (eq 4).[26a] Nonbonded interactions between the chiral auxiliary cyclohexyl group and the $Me_2SiCp''$CpLn portion of the complex are minimized when the (*S*)-epimer adopts a *syn* (**17**, $^i$Pr "back") orientation of (−)-menthyl and when the (*R*)-epimer adopts an *anti* (**18**, $^i$Pr "forward") orientation (eq 4). The *anti* orientation, however, introduces the greatest nonbonded interactions between the isopropyl group and the Ln$(\mu\text{-Cl})_2$Li$(S)_2$ group, as was also observed in the present crystal structure of **2b**.

Since complex **2b** is isolated from diethyl ether solutions and contains (*R*)-(−)-menthylCp with an *anti* orientation of the cyclohexyl ring (Figures 2 and 3), it is likely that the aforementioned solvent effect is again operative and that the stereochemistry of the $Me_3SiCp$ ligand does not strongly influence the R*Cp attachment mode. The observation of three initial diastereomers in THF solutions of crude **2** suggests that structural changes occur in THF that form significant quantities of one or more *rac* diastereomers (**11** or **12**). By analogy to Cp′$_2$YCl·THF,[13c] dissolution of **2** in THF may displace LiCl by THF in the $Ln^{3+}$ coordination sphere. Since coordinated THF would occupy more space in the coordination sphere than chloride, such a substitution would likely destabilize the *anti* R* orientation of the (*R*)-epimer with respect to the *syn*-oriented (*S*)-epimer and thereby reverse the order of diastereomer stability. Epimerization of the $Me_3SiCp$ attachment mode, on the other hand, is less likely to proceed with significant selectivity because the symmetry of the $Me_3Si$ group renders this ring enantiotopic.[3b] Because diethyl ether is much less effective than THF in solvating LiCl, and presumably sufficiently bulky that it cannot effectively compete for a site in the $Ln^{3+}$ coordination sphere, the $MCl_2Li$ unit remains intact in this solvent, resulting in the high observed *meso* selectivity.

**Catalytic Enantioselective Olefin Hydrogenation. Kinetics and Mechanism.** The maximum observed turnover frequency for the hydrogenation of 2-phenyl-1-butene catalyzed by **3a** ($N_t = 860$ h$^{-1}$; $[Ln]_T = 0.938$ mM; $P_{H_2} = 700$ Torr) is 1 order of magnitude smaller than for the same reaction mediated by chiral catalysts derived from $Me_2SiCp''$(R*Cp)LnCH$(SiMe_3)_2$ under similar reaction conditions (cf.: $N_t = 9\,000$ h$^{-1}$; R* = (+)-neomenthyl; Ln = Sm; $[Ln]_T = 1.0$ mM; $P_{H_2} = 750$ Torr). A similar relationship exists between the value of $k_{app}$ determined in the present case (Table 5) and the rate constants found for the $Me_2SiCp''$R*CpSm-catalyzed process ($k = 0.097-0.178$ M$^{1/2}$ atm$^{-1}$ s$^{-1}$).[26] Under conditions of high substrate concentration (∼0.8 M), $v_{H_2}/v_{D_2} = 2.2(1)$ is similar to observed kinetic isotope

Downloaded by CARLI CONSORTIUM on June 30, 2009
Published on April 2, 1996 on http://pubs.acs.org | doi: 10.1021/om950871v

effects for the hydrogenolysis of other $d^0$, $f^n$ metal alkyls in solution[26b,55] and on high surface area metal oxide supports.[56] Given the observed sluggishness with which precatalysts **3** proceed toward formation of hydride **4** (*vide supra*), it seems likely that hydrogenolysis of an intermediate alkyl is involved in the turnover-limiting step of the catalytic cycle (*vide infra*). The activity of the present catalytic system is apparently unaffected by the method of catalyst generation; preformed catalyst is comparable in activity to catalyst prepared *in situ*. This response is unlike those of $[Me_2SiCp''(R^*Cp)LnH]_2$[26b] and $[Me_2Si(1\text{-}Me_3Si\text{-}3\text{-}^tBuCp)_2YH]_2$,[25] in which the strong dimerization of the preformed hydride ($k_1 \gg k_{-1}$ in eq 6) severely depresses catalytic activity, or of $[R_2SiCp''CpLn{-}H]_2$[27] where rearrangement of a marginally active ($N_t = 21\ h^{-1}$ for hydrogenation of 1-hexene) hydride to a covalently linked $\mu$-ligand dimer (eq 17) renders the system incapable of turnover. In the

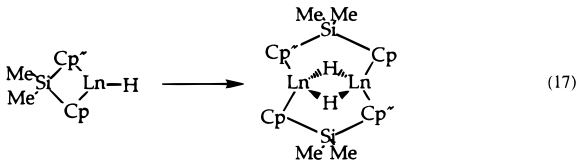


(17)

case of $[Cp'(2,6\text{-}^tBu_2C_6H_3O)YH]_2$, in which a Cp ligand has been replaced by a bulky phenolato group, this effect is so pronounced that the complex exists solely as a symmetrical *trans* $(\mu\text{-H})_2$ dimer ($k_{-1} \approx 0$), even in the presence of a large excess of THF.[29]

The mechanism for the hydrogenation of simple linear and cyclic alkenes catalyzed by $(Cp'_2LnH)_2$ and $(Me_2SiCp''_2LnH)_2$ complexes has been studied in some detail (Scheme 3).[16b] The mechanism involves initial olefin insertion into a Ln−H bond ($k_i$) of the monomer "$Cp'_2LnH$", which is in rapid equilibrium with a hydrido-bridged dimer ($K_{eq}$), forming a hydrocarbyl. Subsequent hydrogenolysis of the intermediate Ln−C bond ($k_p$) regenerates the active "$Cp'_2LnH$" complex with concomitant liberation of alkane. Two limiting kinetic regimes have been identified under typical catalytic conditions: turnover-limiting hydrogenolysis ($k_i$[olefin] > $k_p[H_2]$) and turnover-limiting olefin insertion ($k_i$[olefin] < $k_p[H_2]$). The first scenario usually obtains for simple α-olefins (e.g., 1-hexene) and is described by a rate expression which is zero-order in substrate, first-order in lanthanide, and first-order in $H_2$ pressure (eq 18).

$$v = k[\text{olefin}]^0[\text{lanthanide}]^1[H_2]^1 \qquad (18)$$

Here, olefin capture (insertion) by the metal hydride is rapid and irreversible, essentially displacing the hydride equilibrium entirely to monomer (demonstrated in stoichiometric reactions[13c]), and Ln−C hydrogenolysis is turnover-limiting. The second scenario obtains for more sterically hindered olefins (e.g., cyclohexene), and the rate depends linearly on olefin concentration (eq 19), is half-order in lanthanide, and zero-order in $H_2$. Here, the dimeric hydride[13,16b] is involved in a rapid preequilibrium with a reactive monomer, olefin capture is turnover-limiting, and rapid hydrogenolysis follows this

**Scheme 3. Mechanism for Bis(pentamethylcyclopentadienyl)organolanthanide-Catalyzed Olefin Hydrogenation**

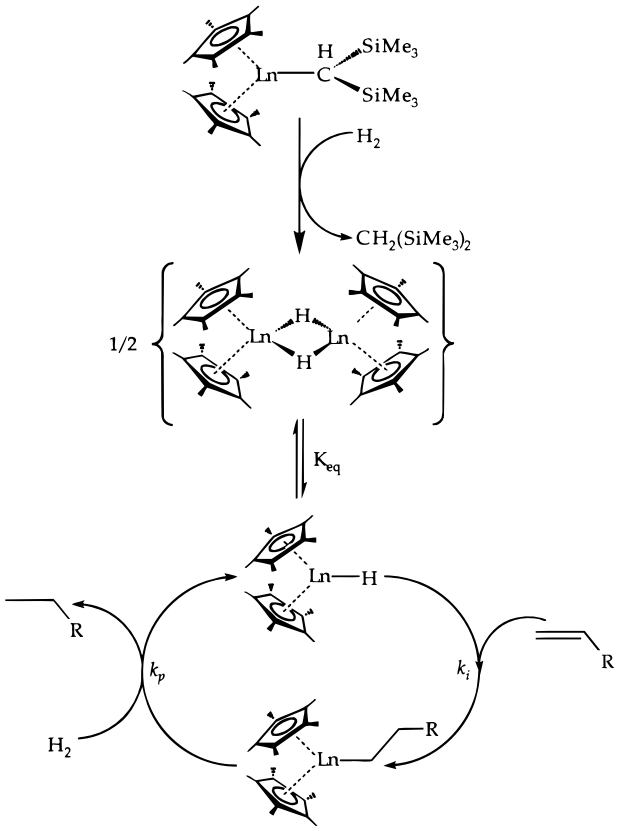


slow step. The hydrogenation of 2-phenyl-1-butene catalyzed by achiral $(Cp'_2SmH)_2$ obeys eq 19, and turnover-limiting olefin insertion is again observed.[26b]

$$v = k[\text{olefin}]^1[\text{lanthanide}]^{1/2}[H_2]^0 \qquad (19)$$

The 2-phenyl-1-butene hydrogenation rate law for $Me_2SiCp''(R^*Cp)Ln$-based catalysts,[26b] on the other hand, does not conform to either of these limiting kinetic scenarios and is shown in eq 20. Hydride, formed by

$$v = k[\text{olefin}]^0[\text{lanthanide}]^{1/2}[H_2]^1 \qquad (20)$$

*in situ* hydrogenolysis of the hydrocarbyl precatalyst, is immediately swept into the catalytic cycle by rapid, irreversible olefin capture. The resulting alkyl, which is in rapid equilibrium with a dialkyl or hydridoalkyl dimer, then undergoes turnover-limiting hydrogenolysis.

The hydrogenation of 2-phenyl-1-butene catalyzed by complex **3a** displays first-order dependence on $H_2$ pressure (eqs 13 and 16), supporting turnover-limiting hydrogenolysis. The significant induction periods—increased ~3x under $D_2$—are consistent with the slow appearance of $CH_2(SiMe_3)_2$ in **3** + $H_2$ $^1H$ NMR experiments (*vide supra*) and indicate sluggishness of Ln−C hydrogenolysis compared to the $Cp'_2$-, $Me_2SiCp''_2$-, and $Me_2SiCp''(R^*Cp)$ analogues. Existing structure/reactivity correlations for this type of organolanthanide complex support a general increase in olefin insertion

(55) Lin, Z.; Marks, T. J. *J. Am. Chem. Soc.* **1987**, *109*, 7979−7985 and references within.

(56) (a) Eisen, M. S.; Marks, T. J. *J. Am. Chem. Soc.* **1992**, *114*, 10358−10368. (b) Gillespie, R. D.; Burwell, R. J.; Marks, T. J. *Langmuir* **1990**, *6*, 1465−1477.

(57) (a) Fendrick, C. M.; Schertz, L. D.; Day, V. W.; Marks, T. J. *Organometallics* **1988**, *7*, 1828−1830. (b) Fendrick, C. M.; Mintz, E. A.; Schertz, L. D.; Marks, T. J.; Day, V. W. *Organometallics* **1984**, *3*, 819−821.

Downloaded by CARLI CONSORTIUM on June 30, 2009
Published on April 2, 1996 on http://pubs.acs.org | doi: 10.1021/om950871v

Downloaded by CARLI CONSORTIUM on June 30, 2009
Published on April 2, 1996 on http://pubs.acs.org | doi: 10.1021/om950871v

reactivity upon opening of the coordination sphere in the equatorial girdle.[15,16,26b,57] However, the deletion of electron-donating ring substituents concomitant with this decrease in steric saturation apparently increases the "hardness" of the ligation or the Ln−C bond enthalpy and depresses the hydrogenolytic reactivity of Ln−C.[29,43] The present formation of oligomeric products during the deuteration of 1-pentene is consistent with these trends.

The observation of half-order dependence on Ln concentration (eqs 13 and 16) suggests a reversible preequilibrium involving dissociation of a dialkyl or hydridoalkyl dimer which precedes turnover-limiting hydrogenolysis.[58] The established tendency of similar coordinatively unsaturated complexes to form polynuclear ($\mu$-H) and ($\mu$-alkyl) species[12,58−60] emphasizes the accessibility of associative processes which may influence reactivity and possibly enantioselectivity (*vide infra*). The exact nature of the present dimer has not been elucidated, although reasonable structures may be postulated by analogy to known chemistry. A doubly-bridged alkyl dimer has precedent in $(Cp_2Ln)_2(\mu\text{-}R)_2$ complexes.[58] The alkyl bridging mode might even involve arene $\pi$ coordination similar to that of $(Cp'_2Sm)_2(\mu\text{-}\eta^2\text{:}\eta^4\text{-}CH_2CHPh)$.[62] Also possible is a $\mu$-hydrido/$\mu$-alkyl dimer such as $(Cp'_2Ln)_2(\mu\text{-}H)(\mu\text{-}R)$. Structurally similar $R_2SiCp''CpLuCH(SiMe_3)_2$ (R = Me, Et) undergoes partial hydrogenolysis to form a structure assigned from NMR as $(Me_2SiCp''CpLu)_2(\mu\text{-}H)[\mu\text{-}CH(SiMe_3)_2]$, a marginally active precatalyst for 1-hexene hydrogenation ($N_t = 21\ h^{-1}$).[27] Formation of the unreactive ring-spanned hydride dimer $Ln_2(\mu\text{-}H)_2(\mu\text{-}R_2SiCp''Cp)_2$ (eq 17) ultimately terminates catalytic activity; however, the crystallographically characterized $Lu_2(\mu\text{-}H)(\mu\text{-}Et)(\mu\text{-}Et\text{-}SiCp''Cp)_2$, formed by reaction with ethylene, supports the accessibility of ($\mu$-H)($\mu$-R) bonding modes.

While the kinetic orders in both [$H_2$] and [Ln] in the present study remain essentially constant through each kinetic trial, the [olefin] dependence is more complex than in any of the previous scenarios and, as noted above, can be divided into two regimes. At high olefin concentration, the rate law is essentially that observed for $Me_2SiCp''$(R*Cp)Ln-based systems (eq 20), i.e., zero-order in olefin, as expected from eq 16. As conversion progresses, the shift to approximately first-order behavior in olefin suggests a concomitant shift to a turnover-limiting insertion mechanism as in eq 19. This implies, however, that the order in [$H_2$] should eventually saturate, which is not observed over the feasable pressure range (*vide supra*), nor does the $H_2/D_2$ KIE decrease. As noted above, $\beta$-elimination/readdition might conceivably become important at lower olefin concentrations; however, it is not detected in isotopic labeling experiments (see Results).

**Scheme 4. Proposed Mechanism for Catalytic Enantioselective Hydrogenation**

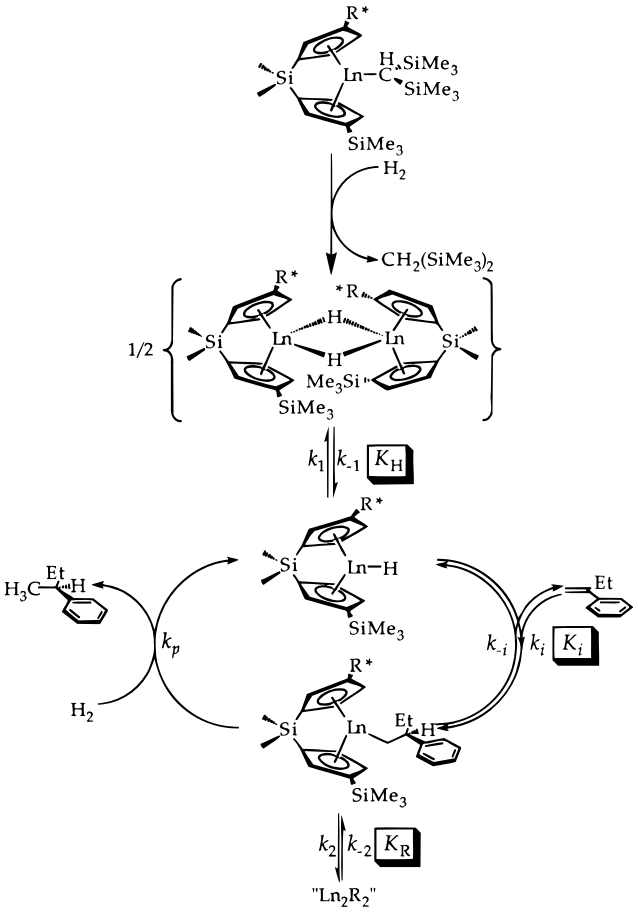


The broadest possible mechanistic scenario for 2-phenyl-1-butene hydrogenation mediated by the present catalysts is shown in Scheme 4. Note the presence of two possible dimer ⇌ monomer equilibria ($K_H$, $K_R$). On the basis of the data at hand, it is impossible to say whether both equilibria are operative or whether (more likely) $K_H$ predominates in low [olefin] regimes and $K_R$ in high [olefin] regimes. The most straightforward way to accommodate the empirical rate law (eq 16) is to divide these regimes. Making the rapid equilibrium approximation,[54] eqs 21−23 yield eq 24 for the low [olefin] regime. At low olefin concentration, it is reasonable that $(LnH)_2$ will be the predominant lanthanide

(58) Although there is no reason in the present case to specifically rule out higher order oligomers, for purposes of discussion the assumption of a dimeric hydrido species is consistent with the observed half-order kinetic behavior and conforms to the well-documented tendency for lanthanocene hydrido and alkyl complexes to favor dimeric forms:[12,13,16,25,29] (a) Holton, J.; Lappert, M. F.; Ballard, D. G. H.; Atwood, J. L.; Hunter, W. E. *J. Chem. Soc., Dalton Trans.* **1979**, 54−60. (b) Holton, J.; Lappert, M. F.; Scollary, G. R.; Ballard, D. G. H.; Pearce, R.; Atwood, J. L.; Hunter, W. E. *J. Chem. Soc., Chem. Commun.* **1976**, 425−426.

(59) (a) Ozawa, F.; Park, J. W.; Mackenzie, P. B.; Schaefer, W. P.; Henling, L. M.; Grubbs, R. H. *J. Am. Chem. Soc.* **1989**, *111*, 1319−1327. (b) Busch, M. A.; Harlow, R.; Watson, P. L. *Inorg. Chim. Acta* **1987**, *140*, 15−20. (c) Waymouth, R. M.; Santarsiero, B. D.; Coots, R. J.; Bronikowski, M. J.; Grubbs, R. H. *J. Am. Chem. Soc.* **1986**, *108*, 1427−1441. (d) Holton, J.; Lappert, M. F.; Pierce, R.; Yarrow, P. I. W. *Chem. Rev.* **1983**, *83*, 135−201. (e) Berry, R. S. *J. Chem. Phys.* **1960**, *32*, 933−938.

(60) (a) Wardell, J. L. In *Comprehensive Organometallic Chemistry*; Wilkinson, G., Stone, F. G. A., Abel, E. W., Eds.; Pergamon Press: Oxford, U.K., 1982; Chapter 2. (b) Fraenkel, G.; Beckenbaugh, W. E.; Yang, P. P. *J. Am. Chem. Soc.* **1976**, *98*, 6878−6885. (c) Witanowski, M.; Roberts, J. D. *J. Am. Chem. Soc.* **1966**, *88*, 737−741. (d) Whitesides, G. M.; Witanowski, M.; Roberts, J. D. *J. Am. Chem. Soc.* **1965**, *87*, 2854−2862.

(61) (a) Schleyer, P. v. R.; Tidor, B.; Jemmis, E. D.; Chandrasekhar, J.; Würthein, E. U.; Kos, A. J.; Luke, B. T.; Pople, J. A. *J. Am. Chem. Soc.* **1983**, *105*, 484−488. (b) Jemmis, E. D.; Chandrasekhar, J.; Schleyer, P. v. R. *J. Am. Chem. Soc.* **1979**, *101*, 527−533. (c) Clark, T.; Schleyer, P. v. R; Pople, J. A. *J. Chem. Soc., Chem. Commun.* **1978**, 137−138.

(62) Evans, W. J.; Ulibarri, T. A.; Ziller, J. W. *J. Am. Chem. Soc.* **1990**, *112*, 219−223.

(63) The insertion is portrayed here as a "1,2" insertion process (Ln delivered to C($\beta$)). The present data, however, are also compatible with a "2,1" insertion which places the electrophilic $Ln^{3+}$ in closer proximity to the arene $\pi$ electron system and is supported by results for organolanthanide-catalyzed olefin hydrosilylation recently reported by this group.[21a]

$$(\mathrm{LnH})_2 \overset{K_1}{\rightleftharpoons} 2\mathrm{LnH} \tag{21}$$

$$\mathrm{LnH} + \text{olefin} \overset{K_2}{\rightleftharpoons} \mathrm{LnR} \tag{22}$$

$$\mathrm{LnR} + \mathrm{H_2} \xrightarrow{k_p} \mathrm{LnH} + \mathrm{RH} \tag{23}$$

$$v = \frac{k_p K_1 K_1[\text{olefin}][\mathrm{H_2}]\{[(\mathrm{LnH})_2] + [\mathrm{LnH}] + [\mathrm{LnR}]\}}{[(\mathrm{LnH})_2]^{1/2} + K_1^{1/2} + K_2 K_1^{1/2}[\text{olefin}]} \tag{24}$$

species present, and plausible $K_1$, $K_2$ scenarios (small $K_1^{1/2}$, $K_2K_1^{1/2}$[olefin]) exist in which the kinetics are half-order in [lanthanide], first-order in [olefin], and first-order in [$H_2$], as observed experimentally. In view of the isotopic labeling results (vide supra), this model requires that $\beta$-H elimination from LnR does not compete effectively with hydrogenolysis. According to this model, as [olefin] increases (departure from this regime), the dependence of the rate on [olefin] will fall toward zero-order (saturation) while the order in [lanthanide] will increase (mass balance and thermochemical considerations argue that [$(MH)_2$] will decrease as [olefin] increases). In the high [olefin] regime,[64] applying the rapid equilibrium model to eqs 25 and 26 and assuming olefin insertion is rapid and irreversible yields eq 28. The orders in [$(LnR)_2$] and [$H_2$] are in agreement with experiment at high [olefin].

$$(\mathrm{LnR})_2 \overset{K_1}{\rightleftharpoons} 2\ \mathrm{LnR} \tag{25}$$

$$\mathrm{LnR} + \mathrm{H_2} \xrightarrow[\text{slow}]{k_p} \mathrm{LnH} + \mathrm{RH} \tag{26}$$

$$\mathrm{LnH} + \text{olefin} \xrightarrow[\text{fast}]{k_i} \mathrm{LnR} \tag{27}$$

$$v = k_p K_1^{1/2}[(\mathrm{LnR})_2]^{1/2}[\mathrm{H_2}] \tag{28}$$

Attempts were also made to derive a single, comprehensive rate law from Scheme 4 using the King−Altman steady-state approach.[54] The resulting expression (eq 29; see Supporting Information for derivation) is some-

$$v = \frac{k_i k_p[\text{olefin}][\mathrm{H_2}][\mathrm{Ln}]_T^{1/2}}{\{2K_H(k_{-i} + k_p[\mathrm{H_2}])^2 + 2K_R k_i^2[\text{olefin}]^2\}^{1/2}} \tag{29}$$

what more complex than those above but also predicts half-order dependence on total lanthanide concentration, as observed experimentally. Importantly, eq 29 correctly predicts the experimentally observed saturation behavior at high [olefin]. It also reveals scenarios where the kinetic dependence on [$H_2$] may fall below 1.0. These include cases of high conversion (low [olefin]) and high (perhaps experimentally unrealized) $H_2$ pressures. Note that there is some evidence for falling [$H_2$] exponent at low olefin concentrations (Figure 9).

As written, Scheme 4 ignores the possibility of noninsertive substrate involvement in the various equilibria and in direct reactions of the various dimers. In regard to the former, it is conceivable that the positions of $K_H$ and $K_R$, hence complete adherence of the kinetic data to eqs 16 or 21−27, could be affected by simple olefin coordination to LnH or LnR monomers. Precedent now exists for complexation to $d^0/f^n$ centers by both exogenous[65a] and "tethered" olefins.[65b,c] In the present system, note that colorless **3a** becomes bright yellow in concentrated 2-phenyl-1-butene solutions and that the color fades upon dilution with aliphatic or aromatic solvents, possibly indicating a weak interaction. Regarding direct hydrogenolytic or olefin insertion reactions of $Ln_2R_2$ and $Ln_2H_2$ species, observations on $R_2SiCp''Cp$-based organolanthanides[27] provide evidence that Ln($\mu$-alkyl)Ln and Ln($\mu$-H)Ln species are unlikely to exhibit catalytically significant reactivity. Regarding hydrogenolysis, the reactivity of $Lu_2(\mu\text{-H})(\mu\text{-Et})(\mu\text{-Et}_2\text{-SiCp''Cp})_2$ is found to be significantly lower than that of even more coordinatively saturated alkyl monomers,[27] suggesting that the contributions of similar species to catalysis are negligible in the present case. Furthermore, while $(R_2SiCp''CpLnH)_2$[27] and $[Cp'(2,6\text{-}{}^tBu_2C_6H_3O)\text{-}YH]_2$[29] insertively accommodate 1 equiv of olefin, arguing that the $Ln_2H_2$ form of the catalyst is not inert toward olefin insertion, the rates are unexceptional and, as noted above, the resulting alkyl does not readily undergo hydrogenolysis.

**Origin of Enantioselection.** Enantioselection in an asymmetric catalytic transformation is determined in the first irreversible step involving diastereomeric transition states.[66] In the mechanism of enantioselective hydrogenation by chiral organolanthanides, it is reasonable that the enantioselective step is olefin insertion into the Ln−H bond. This insertion step is probably operationally irreversible since thermodynamic data indicate $\Delta H \approx -20$ kcal/mol,[64] while the reduction in coordinative unsaturation decreases the likelihood of $\beta$-hydride elimination, as discussed above and argued by the lack of H/D scrambling in deuteration experiments. What remains is to evaluate the origin of enantioselection in terms of both the trajectory and regiochemistry of olefin insertion.

*A priori*, there are at least two trajectories possible for prochiral olefin approach to the organolanthanide center. The first is a lateral approach from the less hindered side of the organolanthanide complex, i.e., the side opposite the *meso*-configured $Me_3Si$ and R* substituents. In the most readily visualized scenario (eqs 30 and 31), the catalyst (*S*,*R*)-epimer should afford (*R*)-2-phenylbutane, with the bulky phenyl group avoiding the larger R* substituent. Exactly the *opposite* situation is observed for the catalytic hydrogenation of 2-phenyl-1-butene with precatalyst **3**. The second trajectory involves olefin approach along the central ring centroid−Ln−ring centroid bisector (eqs 32 and 33) with the Ln−H group bending "back", out of the ring centroid−Ln−ring centroid plane. The central approach accounts well for the observed product stereochemistry in $Me_2SiCp''$(R*Cp)Ln-catalyzed enantioselective hydrogenation,[26b] while molecular mechanics calcula-

(64) (a) Nolan, S. P.; Stern, D.; Hedden, D.; Marks, T. J. *ACS Symp. Ser.* **1990**, *No. 428*, 159−174 and references therein. (b) Nolan, S. P.; Stern, D.; Marks, T. J. *J. Am. Chem. Soc.* **1989**, *111*, 7844−7853 and references therein.

(65) (a) Nolan, S. P.; Marks, T. J. *J. Am. Chem. Soc.* **1989**, *111*, 8538−8540. (b) Casey, C. P.; Hallenbeck, S. L.; Pollock, D. W.; Landis, C. R. *J. Am. Chem. Soc.* **1995**, *117*, 9770−9771. (c) Jordan, R. F.; Wu, Z.; Petersen, J. L. *J. Am. Chem. Soc.* **1995**, *117*, 5867−5868.

(66) Reference 1h, Chapter 1.

Downloaded by CARLI CONSORTIUM on June 30, 2009
Published on April 2, 1996 on http://pubs.acs.org | doi: 10.1021/om950871v

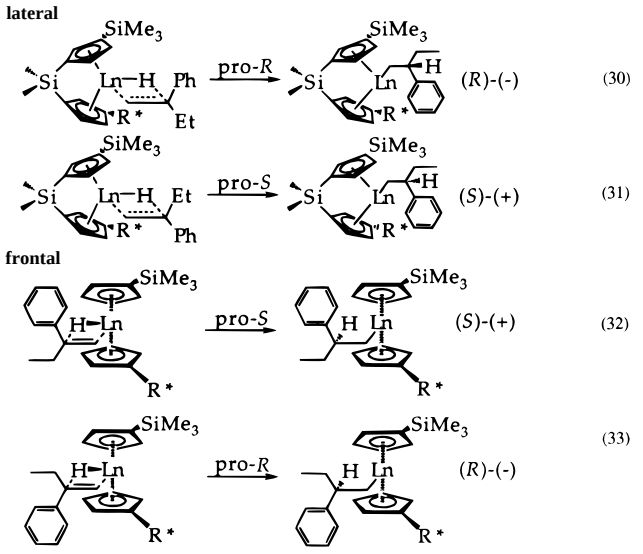


tions[67] and experimental observations[5] support a similar mechanism for olefin insertion into M−H bonds of tetravalent $d^0$ $Cp_2MH(X)$ complexes.

The observed enantioselectivity of the **3**-derived catalysts can be similarly rationalized by examining the central olefin insertion pathways into the Ln−H bond (eqs (32 and 33). A space-filling model of putative monomeric hydride **4a** (Figure 14) reveals the severe dissymmetry of the catalyst in the lateral plane as a result of the *meso*-(*S*,*R*) configuration which plausibly provides effective lateral (**13**, **14**) discrimination in olefin approach and should cause the phenyl and ethyl substituents to orient *anti* to the substituted side of the complex. Discrimination in the transverse plane can be viewed as a result of the differing steric demands of the $Me_3Si$ and (−)-menthyl groups: the $Me_3Si$ group is relatively compact, while the (−)-menthyl group sweeps out a much larger region of space, intruding into the reaction zone on the other side of the ring centroid−Ln−ring centroid plane in such a way as to bias the phenyl group toward the $Me_3Si$ ring substituent. Thus, the template or "pocket" formed by the ligand−metal complex appears to approximate the mirror image of a dissymmetrically 1,1′-disubstituted olefin, such as 2-phenyl-1-butene. In the frontal pro-*S* approach of the olefin (eq 32), the phenyl group is *syn* to the smaller $Me_3Si$ and *anti* to the larger (−)-menthyl group. This model yields the predominant 2-phenyl-1-butene product configuration observed experimentally (Table 4). In the frontal pro-*R* approach (eq 33), the phenyl would make a closer approach to the (−)-menthyl group, leading to a more sterically congested transition state; this is also the case in the lateral pro-*S* approach (eq 31). This situation should be exacerbated on reducing the size of the lanthanide ion (drawing the ligand sphere in more closely), and indeed, the Lu analog **3b** yields products of significantly higher optical purity. This model also explains the observed enantioselectivities for 1-pentene deuteration and 2-ethyl-1-hexene hydrogenation with **3** (Table 4). In the latter case, the steric requirements of the ethyl and butyl substituents are not sufficiently dissimilar for effective enantioselection.

Although olefin insertion is ostensibly the enantioselective step in the catalytic cycle, the low enantioselectivities observed for **3**-catalyzed deuteration of styrene (Table 4) raise questions about pathways for product racemization in these systems. As noted above, the lack of significant H/D scrambling offers little support for $\beta$-elimination−readdition sequences as pathways for racemization (eq 34). However, the present dimeric

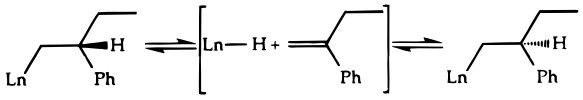


alkyl intermediate and previous observations on organolanthanide $\mu$-alkyls[27] suggests another pathway for racemization within a dimeric form. Racemization could occur through inversion of a bridging 2-butyl carbon (eq 35), as would occur in a 2,1-insertion of 2-phenyl-1-

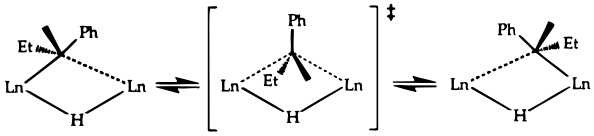


butene into Ln−H.[63] Although this may be a less obvious pathway, the NMR spectra of $Ln_2(\mu\text{-H})(\mu\text{-R})(\mu\text{-R}_2SiCp''Cp)_2$[27] and $(Cp'YOAr)_2(\mu\text{-H})(\mu\text{-R})$[29] indicate an inversion process at the bridging (primary) carbon atom of the $\mu$-R group.

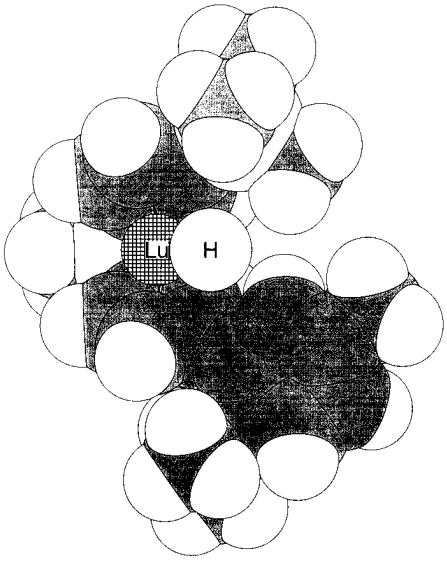


**Figure 14.** Space-filling model of (*S*,*R*)-$Me_2Si(Me_3SiCp)$-[(−)-menthylCp]LuH. The metal−ligand template was constructed from the diffraction-determined atomic coordinates of complex **2b**.

## Conclusions

Organolanthanide complexes of the new chelating ligand $Me_2Si(3\text{-}Me_3SiCp)[3\text{-}(-)\text{-menthylCp}]^{2-}$ are the first examples of a *meso* metallocene framework in organo−group 3/−lanthanide chemistry. Such a configuration induces gross distortions of the idealized $C_{2v}$ symmetry observed in previously characterized lanthanocenes, both achiral and chiral. Due to the significantly reduced steric requirements of the ancillary ligation in the present case, rotoisomerism involving the $Ln-CH(SiMe_3)_2$ bond, normally suppressed in more sterically demanding $Cp'_2Ln$ environments, is visible in the NMR of the hydrocarbyl derivatives. The *meso*

(67) Lin, Z.; Marks, T. J. *J. Am. Chem. Soc.* **1990**, *112*, 5515−5525 and references therein.

Downloaded by CARLI CONSORTIUM on June 30, 2009
Published on April 2, 1996 on http://pubs.acs.org | doi: 10.1021/om950871v

metal−ligand template offers surprisingly high enantioselectivities when these precatalysts are employed in the asymmetric hydrogenation or deuteration of both styrenic and non-styrenic olefins. The kinetic behavior of **3a**, however, is unlike that of more coordinatively saturated lanthanocenes, illustrating how the perturbation of ancillary ligand steric and electronic properties significantly modulates the relative rates of dimerization, insertion, and hydrogenolysis, which, in turn, opens mechanistic pathways previously unobserved in any one organolanthanide catalyst system.

**Acknowledgment.** We thank National Science Foundation for generous support of this research under Grant CHE9104112. We thank Professor Harold Kung for suggestions regarding the kinetic derivation and Professor Paul Loach for access to his CD spectrometer.

**Supporting Information Available:** A crystal structure report, tables of positional and thermal parameters, and text and equations for the derivation of rapid equilibrium and steady-state kinetic expressions (14 pages). Ordering information is given on any current masthead page.

OM950871V

Downloaded by CARLI CONSORTIUM on June 30, 2009
Published on April 2, 1996 on http://pubs.acs.org | doi: 10.1021/om950871v